

UC Berkeley

UC Berkeley Electronic Theses and Dissertations

Title

Kinematic Correlates to Behavioral Outcomes and Effects of Caloric Inadequacy in Traumatic Brain Injury in Rats

Permalink

<https://escholarship.org/uc/item/27d07721>

Author

Peck, Austin J

Publication Date

2020

Peer reviewed|Thesis/dissertation

Kinematic Correlates to Behavioral Outcomes and Effects of Caloric
Inadequacy in Traumatic Brain Injury in Rats

by

Austin J Peck

A dissertation submitted in partial satisfaction of the

requirements for the degree of

Doctor of Philosophy

in

Integrative Biology

in the

Graduate Division

of the

University of California, Berkeley

Committee in charge:

Professor George A. Brooks, Chair
Professor Daniela Kaufer
Professor Jose Pablo Vazquez-Medina
Professor Gregory W. Aponte

Fall 2020

Kinematic Correlates to Behavioral Outcomes and Effects of Caloric
Inadequacy in Traumatic Brain Injury in Rats

Copyright 2020
by
Austin J Peck

Abstract

Kinematic Correlates to Behavioral Outcomes and Effects of Caloric Inadequacy in Traumatic Brain Injury in Rats

by

Austin J Peck

Doctor of Philosophy in Integrative Biology

University of California, Berkeley

Professor George A. Brooks, Chair

Traumatic brain injury (traumatic brain injury (TBI)) accounted for 2.88 million Emergency Department Visits Hospitalizations and Deaths (EDHDS) in the USA alone in 2014, not accounting for the many sub-clinical injuries that are often unreported and untreated. A vast majority of these injuries are closed head TBI involving direct contact with the skull and rapid acceleration / deceleration events. While a variety of experimental TBI models exist, most succeed at either reproducing specific mechanisms of injury or specific gross and molecular consequences (diffuse axonal injury, reactive astrogliosis, etc), but not always both. In this work, I highlight a free rotation closed-head traumatic brain injury (FRCHTBI) model that mimics the mechanisms of impact most common in human injuries. Even in high risk scenarios, kinematic information from instrumented equipment or video analysis is typically the best case scenario for quantifying the impact event. As such, I highlight a method for measuring kinematic properties (linear and angular accelerations of the head) in this model using only a high speed camera, as well as an example of behavior analysis taking into account sources of variation common in these models (Chapter 2).

Detection of acute, sub-acute, and chronic deficits are crucial to tying behaviorally measured affects of TBI models to their anatomical and molecular consequences, and evaluate efficacy of interventions. In chapter 3, I present a pair of rodent behavioral assays with low barriers to implementation and high clinical significance. The light aversion assay (LAV) is an adaptable measure of photosensitivity, a commonly reported symptom in mild to severe TBI, that can be optimized to detect various severities, and was able to detect differences in very mild TBI 14 days after injury. Gait analysis using open source software and walkway plans was also effective at detecting changes in temporal (stance and swing phase) and spatial (step length) gait parameters 30 min post impact.

Lack of appetite is commonly reported following mild to severe TBI, and patients in the neuro intensive care unit (ICU) have been shown to be in highly catabolic states under the current standard of care, indicating inadequate caloric support to repair the injured brain. Despite its involvement across all severities of injury, few studies focus on nutritional interventions following TBI. In chapter 4 I explore a rat TBI adequacy-inadequacy model with and without sodium lactate (NALAC) supplementation as a potential means of exploring the interplay between caloric sufficiency and lactate supplementation. However, with the impact parameters used in the present study a very mild TBI was induced, below the detection threshold of several commonly used tests. This unfortunately was not a sufficient level of injury to evaluate group differences for the nutritional model introduced.

Collectively, this work explores clinically relevant methods related to many stages of rodent TBI studies including injury induction (chapter 2), severity detection and outcome evaluation (chapter 3), and experimental nutritional interventions (chapter 4).

To my grandparents who are no longer with us in mind or body.

I know how much this would have meant to you, and I share it with you in spirit.

Contents

Contents	ii
List of Figures	iv
List of Tables	v
1 Introduction	1
1.1 TBI	1
2 Behavioral and Kinematic Analysis in a Rat FRCHTBI Model Using High Speed Video Tracking	4
2.1 Abstract	4
2.2 Introduction	4
2.3 Methods	6
2.4 Results	9
2.5 Discussion	11
2.6 Conclusion	12
2.7 Figures	13
3 Light Aversion and Gait Analysis as Low Cost, Clinically Relevant Assays for Murine TBI Evaluation	20
3.1 Abstract	20
3.2 Introduction	21
3.3 Methods	22
3.4 Results	26
3.5 Discussion	28
3.6 Conclusion	31
3.7 Figures	32
4 Caloric Adequacy and Behavioral Outcomes in a Rat FRCHTBI Model	39
4.1 Abstract	39
4.2 Introduction	39
4.3 Methods	40

4.4	Results	43
4.5	Discussion	46
4.6	Conclusion	49
4.7	Figures	50
5	Conclusions and Future Directions	60
	Bibliography	62

List of Figures

2.1	Drop-weight bolt-transfer FRCHTBI apparatus with inlay of breakaway platform	14
2.2	Point tracking and kinematic traces of a representative impact	15
2.3	Distribution of kinematic measurements and impact properties for 450g, 135cm, 3cm	16
2.4	Impact properties and beam-walk performance	17
2.5	Impact properties and inverted wire mesh performance	18
2.6	Impact properties and delta time in center of arena and delta distance traveled for open field	19
3.1	Light aversion assay optimization	32
3.2	Light aversion assay TBI detection validation	33
3.3	Likelihood filtering improves accuracy of tracked body part data	34
3.4	Temporal and spatial representation of stance phases from a single pass	35
3.5	Stance phase increased in TBI animals	36
3.6	Swing phase increased in TBI animals	37
3.7	Step length decreased in TBI animals	38
4.1	Experimental Timeline	50
4.2	Daily bodyweight and food consumption	51
4.3	Open field performance by group over time	52
4.4	Beam-walk performance by group over time	53
4.5	Hanging time on inverted wire mesh	53
4.6	Elevated plus maze performance 10 days post TBI	54
4.7	Barnes table maze performance 11 - 13 days post TBI	55
4.8	Light aversion assay performance 14 days post TBI	56

List of Tables

2.1	Kinematic measurements and injury properties with varied injury input parameters	13
4.1	Daily change in bodyweight pre, 24 after, and post impact	57
4.2	Daily food consumption pre, 24 after, and post impact	58
4.3	Daily change in food consumption pre, 24 after, and post impact	59

Acknowledgments

My advisor and thesis committee: As I reflect on my time here, I realize how much you have each impacted my life and what I have gained from this experience.

Professor Brooks: Much of the knowledge gained about science and myself during my time in your lab extends well beyond the content of this dissertation. For these opportunities to explore and grow, I am sincerely grateful.

Professor Kaufer: Meetings with you never felt long enough. Your scientific input and expertise were invaluable at many stages throughout the years. Your warmth and ability to be truly present always held the potential to change a day for the better.

Professor Vazquez-Medina: Your passion and commitment to science is contagious, and I can already see the impact it has had on members of your lab and beyond. I am grateful for your generosity with your time and expertise. My only regret in working with you is that it was for such a short time.

Professor Aponte: This thesis and my scientific training have benefited significantly from your thoughtful feedback and contributions. You always questioned assumptions and expected clear justification for each decision. Anticipating these questions made my work more thorough, and I strive to approach aspects of my life more thoughtfully as a result.

Jose Arevalo: I'm not sure what this project would have been like without your help, but I'm glad I didn't have to find out. Your reliability, curiosity, and input made it possible. Your company, humor, and friendship made it bearable.

Chi-An Emhoff: Your willingness to entertain (way too many) questions about exercise physiology research from an undergraduate on a weekly basis played a significant role in my choice to pursue a higher degree. Nearly a decade later, I still value your continued mentorship and friendship.

The many undergraduates and facility staff who have helped along the way: This truly would not have been possible without you, and I am grateful for your hard work and commitment.

This work was generously funded by the Pac-12 Student Athlete Health & Well-Being Initiative (Pac-12 CAL-Brooks-17-02).

For my family, who keep asking "When will you finally be done with school?": I am done.

My close friends, in Berkeley and beyond: Thank you for bringing much needed balance to my graduate experience, for bearing with me during periods when stress boiled over, and for serving as a team of untrained psychologists at the most challenging points.

Mom and Dad: I would never have embarked down the path that led me to this moment if you hadn't stressed the importance of curiosity and education (you probably should have mentioned I was supposed to get a job at some point though). The older I get the more I recognize and appreciate the sacrifices you each made for my benefit. Thank you, and I love you.

Tater: Thank you for the chair-side company and for reminding me to take the occasional writing break. There will be more time for walks now, I promise.

Marianne Brasil: Have I mentioned recently that you're a catch? Words cannot express the ways you have improved every aspect of this experience. I respect you tremendously as a scientist, and value you immensely as a partner. High five! I like!

Chapter 1

Introduction

1.1 TBI

According to the National Institute of Neurological Disorders and Stroke (NINDS), traumatic brain injury (TBI), a form of acquired brain injury, occurs when a sudden trauma causes damage to the brain while the Centers for Disease Control (CDC) defines TBI as an injury caused by a bump, blow, or jolt to the head that disrupts the normal functions of the brain. This broad definition encompasses a variety of physical causes, time courses and clinical manifestations of symptoms, and outcomes. The complex presentation of TBI make developing definitive guidelines for evaluation and treatment difficult (Bazarian et al., 2005; Hyder et al., 2007), highlighting the importance of improving our understanding of the molecular, neurocognitive, and metabolic sequelae and specific deficit detection.

The CDC reported a 53% increase in TBI related EDHDS between 2006 (1.88 million) and 2014 (2.88 million) in the USA (CDC, 2019). While these injuries were present across all demographics, adults aged 75 and older had the highest per capita EDHDS (CDC, 2019), which is especially important as the proportion of adults aged 65+ and median population age is projected to continue increasing in the coming decades (Sanderson et al., 2017). High prevalence in children and young adults is an equally concerning trend with long term consequences. Evidence increasingly suggests that TBI affects normal cognitive development and aging, increasing the likelihood of developing neurodegenerative diseases such as Alzheimer's and Parkinsons disease, and predisposing them to long term neurological disability (Bramlett and Dietrich, 2015; Daneshvar et al., 2011; Masel and DeWitt, 2010). Even asymptomatic athletes as young as high school with accumulation of mild traumatic brain injury (mTBI) can begin to show cognitive impairment and deficits in blood brain barrier (BBB) function (Amyot et al., 2018; Talavage et al., 2014; Veksler et al., 2020).

Perhaps less obvious than negative health and quality of life outcomes, the fiscal impact of TBI is immense. It is estimated that the annual TBI related economic burden in the US

alone was \$60 billion spread across treatment, rehabilitation, and lost productivity (Finkelstein et al., 2006). A forecast by Corso et al. (2006) highlights the fiscal implications of the long term neurological effects of TBI, attributing 326 billion of the 406 billion in lifetime costs from TBI occurring in 2000 to lost productivity.

Physical mechanisms of TBI are typically classified as closed head, penetrating, or blast injuries. While blast injuries are becoming increasingly common within members of the armed forces exposed to explosive devices, they are fairly uncommon within the civilian population (Rosenfeld et al., 2013). Penetrating injuries, caused by foreign objects penetrating the skull and causing direct damage to brain tissue, are significantly less common than closed head injuries, but are a leading cause of TBI related death and tend to have poor prognosis (Alao and Waseem, 2020; Vlček et al., 2018; CDC, 2019). Closed head injury is by far the most common form of TBI (CDC, 2019; Kumar and Loane, 2012). These often involve both the direct transfer of energy through blunt force trauma and rapid acceleration / deceleration events, most commonly caused by falls or being struck by or against an object (CDC, 2019; Faul and Coronado, 2015).

In order to understand treatment and prevention of each cause of injury TBI research models have become similarly homogeneous, requiring the development of a range of experimental models that aim to either mimic varied mechanical causes of TBI or reproduce specific symptoms and activation of molecular pathways observed in clinical cases (Namjoshi et al., 2013). Despite being designed to reproduce specific injury properties, some of the most widely used TBI models, controlled cortical impact (CCI) and fluid percussion injury (FPI), require surgical removal of the skull to make direct impact with the cortical surface (Feeney et al., 1981; Dixon et al., 1987; McIntosh et al., 1987; Dixon et al., 1991; Smith et al., 1995). Newer models have emerged aiming to reproduce the gross and molecular properties of human TBI using impacts that also reproduce similar physical properties of more common closed head injuries, including the model used in this work (Foda and Marmarou, 1994; Kane et al., 2012; Marmarou et al., 1994).

Cerebral metabolism can be altered for days, weeks, or even months following TBI (Giza and Hovda, 2014; Passineau et al., 2000), and is especially worrisome for individuals with post concussive syndrome and those at risk of exposures to multiple impacts (Vagnozzi et al., 2007, 2008; Prins et al., 2013). Hypertonic lactate infusion therapy is a promising addition to treatment for TBI that serves to reduce inflammation and intracranial pressure (Bouzat et al., 2014), serve as a preferred fuel source for the brain (Glenn et al., 2015a; Schurr, 2006), and spare the brain and bodys glycogen stores by serving as a precursor for gluconeogenesis (GNG) (Glenn et al., 2015b). However, data regarding supplementation in the most common form of TBI (closed head mTBI) is mixed, and has not included lactate (except possibly in studies with proprietary formulas). Several products are marketed as supplementation for concussion prevention and recovery, but human data supporting these claims is limited (Ashbaugh and McGrew, 2016; Trojian et al., 2017). However, some animal studies

have reported improved behavioral, structural, and inflammatory outcomes (Sullivan et al., 2000; Yu et al., 2018).

In the following chapters I include methods for analysis of FRCHTBI induction and outcome analysis, as well as an experimental model of nutritional inadequacy following TBI. Chapter 2 presents a method for evaluating impact consistency in murine FRCHTBI models using high speed image capture and incorporating inherent variation into outcome analysis. Chapter 3 presents two assays designed to allow more labs to assess clinically relevant TBI measures (photosensitivity and gait patterns) in rodent models using freely available open source software and readily available materials. Chapter 4 outlines the results from an experimental model exploring the effect of nutritional adequacy on outcomes in TBI. Chapter 5 synthesizes the collective results of the previous chapters and highlights their utility for future TBI research.

Chapter 2

Behavioral and Kinematic Analysis in a Rat FRCHTBI Model Using High Speed Video Tracking

2.1 Abstract

Many open skull traumatic brain injury (TBI) models include ways to precisely modulate and quantify targeting and forces involved in injury induction, which the most widely used closed-head injury (CHI) TBI models lack. We present a method for analyzing kinematic properties in free rotation closed-head traumatic brain injury (FRCHTBI) impacts using high-speed (1,000 FPS) video recording and open-source motion tracking software. This set of tools can be deployed to quantify linear and angular velocity and acceleration, which correlate to injury severity in human TBI, regardless of impact apparatus. Variation in targeting and transfer of force inherent in FRCHTBI models can be a strength when modeling the human condition, but only if these sources of variation are appropriately quantified to contribute to analysis.

2.2 Introduction

The the Centers for Disease Control (CDC) reported 2.88 million Emergency Department Visits Hospitalizations and Deaths (EDHDS)s in the US in 2014, not accounting for the many subclinical instances of TBI going unreported or untreated (CDC, 2019; Langlois et al., 2006; Bazarian et al., 2005). Mounting evidence suggests that TBIs can cause long term deficits, and serve as an independent risk factor for many neurological consequences including general cognitive decline, epilepsy, stroke, and dementia (Wilson et al., 2017; Roozenbeek et al., 2013; Veksler et al., 2020). As a result, TBIs incur an enormous emotional and fiscal cost to individuals, the healthcare system, and the economy as a whole

(Bramlett and Dietrich, 2015; Finkelstein et al., 2006; Corso et al., 2006; Maas et al., 2017).

Because real world TBIs are unique and varied in their cause, severity, and symptoms, a number of animal models exist to reproduce the various mechanisms of injury or specific aspects of the pathophysiology (Namjoshi et al., 2013; Ma et al., 2019; Albert-Weissenberger and Sirén, 2010). Several of the most widely adopted injury models (namely controlled cortical impact (CCI) and fluid percussion injury (FPI)) require a craniotomy to apply a precise force directly to the surface of the brain, resulting in primarily focal injury characteristics (Feeney et al., 1981; Dixon et al., 1987; McIntosh et al., 1987; Dixon et al., 1991; Smith et al., 1995). However, a vast majority of TBIs are closed head impacts with diffuse injury largely contributing to outcomes (CDC, 2019; Maruichi et al., 2009).

In many closed-head traumatic brain injury (CHTBI) studies the animals head rests on a foam pad which relies on consistent mechanical properties of the foam pad to produce reliable injury outcomes, increased instances of skull fracture, and can lead to secondary impacts (Bodnar et al., 2019). Some such models additionally induce diffuse injuries often seen in CHTBI by distributing impact force across a metal disc secured to the exposed skull (Maruichi et al., 2009). Few instances of human TBI are skull crush, and they tend to present a unique set of symptoms (CDC, 2019; Gonzalez Tortosa et al., 2004). Free rotation closed-head traumatic brain injury (FRCHTBI) models, such as the modified Marmarou model, involve unrestricted acceleration/deceleration and rotation that better reproduce the mechanical properties across a spectrum of mild to severe human TBIs (eg mild sport impacts to motor vehicle accidents) (Kane et al., 2012; Marmarou et al., 1994; Foda and Marmarou, 1994).

Many commonly-used CHTBI models utilize a falling weight to deliver a blow to the head (Albert-Weissenberger and Sirén, 2010). This approach can lack precise control over targeting and force applied and lead to variability from impact to impact, even within the same reported input parameters (Namjoshi et al., 2013). Because many investigators do not capture or report these sources of variation in their work, it can be difficult to guarantee consistent injuries and reproduce outcomes. This is especially true between labs with different injury induction apparatuses. In the real world, TBIs do not have precisely controlled inputs, so these variations in impacts can be leveraged to better understand the aspects of a FRCHTBI that best predict injury severity.

Analysis of human head impacts using equipment fashioned with inertial measurement unit (IMU)s have identified that linear acceleration (LA), angular acceleration (AA), and site of impact are predictive of outcome (Rowson et al., 2012; Kleiven, 2013). The technique described here takes data similar to that collected by this instrumented equipment without designing miniaturized versions. By focusing on targeting of impact and kinematic properties post impact we can better understand how these variables affect the gross brain anatomy, cellular and molecular consequences, and secondary injury cascades. This TBI

device agnostic suite of tools allows researchers to correlate their impact outcomes to human relevant kinematic metrics (linear acceleration and angular acceleration) in FRCHTBI animal models using only a high-speed camera (1000 FPS+).

2.3 Methods

Animal Care

All animal procedures were approved by the Animal Care and Use Committee (ACUC) at the University of California Berkeley. Male Sprague Dawley rats were purchased from Charles River USA (Wilmington, MA) at 49 days of age and housed individually. Cages were maintained at a constant temperature and humidity with a 12 hour light-dark cycle (light 7:00 am to 7:00 pm) with ad lib access to food and water.

TBI Apparatus

A rail-guided bolt force-transfer weight drop apparatus (Figure 2.1 A) (Orendorff et al., 2017) was used to induce a FRCHTBI similar to the Wayne State modified Marmarou method (Kane et al., 2012; Marmarou et al., 1994; Foda and Marmarou, 1994). A hex bolt rests on the animals head and transfers energy from the falling weight to the targeted location. The foil break-away platform (Figure 2.1 B) was modified by fitting a U - shaped acrylic platform to rest inside the box with a 2 cm protruding ledge allowing rubber tipped spring clamps to hold consistent tension without obstructing the cameras field of view throughout the post impact events. Perforations were made along the mid-line of the platform using a circular saw blade and guide to limit variation in foil scoring and break-away resistance from impact to impact.

Injury Induction

Prior to impact, an anesthetic state was induced using 3.5% isoflurane atomized in oxygen at a flow rate of 1 L/min. At 5 minutes animals were removed to mark the fur with a non-toxic water soluble marker superficial to the proximal edge of the mandible, scapula, and ilium, then returned to the chamber until the continually running timer reached 10 minutes. If breathing rate remained elevated or toe-pinch reflex was present animals were returned for an additional minute. Animals were then quickly moved to a perforated foil platform 8 cm above a 7.6 cm thick medium-density foam pad in a prone position. The bolt was positioned on the rat's head along the midline and aligned with the ears to target between lambda and bregma. After confirming the toe-pinch reflex had not been regained, the weight was released from the appropriate height. Sham animals underwent the same course of anesthesia and placement on the apparatus with no weight drop. Immediately post impact, animals were returned to a clean cage in the supine position and observed.

High-Speed Videography and Motion Tracking

Impacts were filmed along the sagittal plane at 1,000 FPS using an X-PRI model camera from AOS Technologies (Switzerland) and saved to contain several frames prior to impact and after the animal comes to rest. Frame by frame positional data for marked points were analyzed using open-source software point tracking software Tracker (Douglas Brown, V5.0.5).

Varying Input Parameters

To demonstrate application of our method to TBI optimization, we systematically changed input variables relevant to our TBI apparatus and compared the resulting impact kinematics. Impacts were administered with combinations of impactor weight (610, 450, 305 g), bolt throw - the distance available for the impactor to transfer energy to the bolt - (1, 3, 4.5 cm), and drop height (67.5, 135 cm) to understand the effect of each. Comparisons were also made between rats of various weights (219 to 594 g) under the same impact conditions (450g, 3 cm, 135cm).

Variation in Targeting and Bolt Throw

Bolt throw was calibrated for each day of impacts and when throw settings were adjusted using a sham animal. A pre-impact frame from each video was chosen and a reference object of known length in the same plan as the animal was used to calibrate pixels to real world units of distance using ImageJ (Schneider et al., 2012). To quantify variation in throw due to differences in animal anatomy, animal placement, and variations in foil platform tension, the distance between the top surface of the bolt and the top of the stopper platform was reported. To quantify variation in targeting within and between groups of animals receiving the same impact parameters, the distance from the distal corner of the rat's eye to the midline of the bolt was reported.

Kinematic Calculations

Kinematic calculations and analysis were primarily undertaken by a collaborator. Details relevant to the present chapter are briefly described below, with further detail covered in an forthcoming work (Gleason and Peck, in preparation). Filtered frame by frame positional data for the eye and ear from video tracking is used to calculate instantaneous linear and angular velocities and accelerations throughout the time course of the impact using rigid body mechanics. Pixel values were calibrated to real world units by a scale bar visible in frame of the video, and peak values for each parameter were recorded for use in the present study.

Behavior assessments

open field (OF), beam-walk (BW), and inverted wire mesh (IWM) tasks were used to evaluate a subset of animals receiving impacts of 450 g, from 135 cm, and 3 cm throw for short term deficits by measuring performance pre and 30 min post impact. All tasks were recorded for later scoring by behavior analysis software (OF) or reported as the average and standard deviation of 3 scorers blinded to the animals condition (BW and IWM).

Beam-Walk

The BW apparatus was a 3.8 x 128 cm textured acrylic beam with an open 20 x 16.5 x 14 cm (depth x width x height) dark box at one end mounted 90 cm above the floor with a tarp was draped below the beam to prevent potential fall injuries. For each trial, rats were placed at the open end facing the dark box and given up to 45 seconds to traverse the beam until entering the box or falling. For two days prior to impact rats were trained on the task until they could complete the task in less than 45 seconds without assistance (up to four trials per day). Animals were allowed to remain in the box for 30 seconds as reinforcement after completing the task, and were guided to the box for reinforcement if they did not complete the task in the allotted time. Trials were recorded and scorers were blinded to animal status. Time for the animals nose to enter the box, number of foot faults, partial falls (two limbs off, but recovered), and falls were scored.

Open Field

Rats were placed in the center of the OF arena measuring 58 x 58 cm and allowed to explore undisturbed for 1 min. Videos were analyzed using Ethovision 15 (NOLDUS; Leesburg, VA) where a 37 x 37 cm center zone and 10.5 x 10.5 cm corner zones were defined. Distance traveled and time in center zone was recorded and difference between pre impact and post impact values were reported.

Inverted Wire Mesh

Two acrylic frames with external dimensions of 45 x 45 cm and internal dimension of 35 x 35 cm were fastened by bolts to secure 1.25 cm wire mesh for the testing arena. Rats were placed in the center of the wire mesh and once all 4 paws were secure, the arena was inverted by flipping animal head-over-tail over a draped tarp. Time from inversion to release was recorded.

Statistical Analysis

Statistical analysis was performed using python module statsmodels v0.12.1 (Seabold and Perktold, 2010) in python v3.7.7 (Python Software Foundation, <https://www.python.org/>). Values were reported as mean \pm SD. Correlation of injury and behavior parameters was

tested using ordinary least squares regression and testing for non correlation. Correlations were considered significant with $\alpha < 0.05$ and noted as approaching significance with $\alpha < 0.1$.

2.4 Results

Video Tracking and Kinematic Calculations

Figure 2.2 shows a representative point tracking for 5 segments of an impact video spanning 500 ms from the 450 g, 135 cm, 3 cm group from immediately pre-impact (1) until just before the animal comes to rest on the foam pad (5) (top panel), a composite of the complete tracking path with the rats position at each of the frames visible and labeled (middle panel), and the resulting frame by frame values for linear and angular velocity and acceleration with the time points of frames 1 - 5 indicated (bottom panel). From these values, the peak of absolute values of each kinematic measurement was extracted and recorded for the work in this chapter. Further analysis of kinematic properties and profiles of each injury will be the topic of my colleagues work.

Variation in Kinematic and Injury Parameters

Peak values for linear and angular velocity and acceleration were calculated in this way for 39 impact to explore the effect of varying impact settings for this particular TBI apparatus. Drop weight (305, 450, and 610 g), drop height (67.5, 135 cm), and intended bolt throw (1, 3, 4 cm) were manipulated, resulting in 8 distinctive combinations of impact settings (305 g, 135 cm, 3 cm ($n = 3$); 450 g, 135 cm, 3 cm ($n = 18$); 450 g, 135 cm, 4 cm ($n = 3$); 610 g, 67.5 cm, 1 cm ($n = 3$); 610 g, 67.5 cm, 3 cm ($n = 2$); 610 g, 135 cm, 1 cm ($n = 3$); 610 g, 135 cm, 3 cm ($n = 4$); 610 g, 135 cm, 4 cm ($n = 3$)). Table 2.1 reports the mean and standard deviation of rat weight, measured bolt throw, bolt targeting, and kinematic measurements for each group.

To evaluate how changing impact settings on the current apparatus affected kinematic measurements, peak values for linear and angular velocity and acceleration were calculated in this way for 39 impact to explore the effect of varying impact settings for this particular TBI apparatus. Drop weight (305, 450, and 610 g), drop height (67.5, 135 cm), and intended bolt throw (1, 3, 4 cm) were manipulated, resulting in 8 distinctive combinations of impact settings (305 g, 135 cm, 3 cm ($n = 3$); 450 g, 135 cm, 3 cm ($n = 18$); 450 g, 135 cm, 4 cm ($n = 3$); 610 g, 67.5 cm, 1 cm ($n = 3$); 610 g, 67.5 cm, 3 cm ($n = 2$); 610 g, 135 cm, 1 cm ($n = 3$); 610 g, 135 cm, 3 cm ($n = 4$); 610 g, 135 cm, 4 cm ($n = 3$)). Table 2.1 reports the mean and standard deviation of rat weight, measured bolt throw, bolt targeting, and kinematic measurements for each group.

To determine how consistent kinematic and impact properties were with the same settings, 18 animals received impacts of a 450 g weight from 135 cm with 3 cm bolt throw and

distribution of angular acceleration, linear acceleration, bolt target, and measured bolt throw were recorded (Figure 2.3). For this set of impacts angular acceleration averaged $33,596 \pm 12,270$ and ranged from 19,563 - 66,162 rad/s^2 (A) and linear acceleration averaged 534 ± 41.7 and ranged from 469 - 620 m/s^2 (B). Bolt targeting ranged averaged 1.64 ± 0.19 and ranged from 1.23 - 1.96 cm from the nose (C) and measured bolt throw averaged 2.42 ± 0.49 and ranged from 1.6 - 3.2 cm (D).

Impact and Behavior Correlations

A subset of the animals receiving impacts of a 450 g weight from 135 cm with 3 cm bolt throw had their performance on 3 behavioral tasks measured 30 minutes after TBI to see if there was correlation between injury properties and performance within a single set of impact settings. Angular acceleration and linear acceleration represent the kinematic injury measures and bolt target and measured bolt throw represent impact properties. Behavior performance measures varied by task.

Beam-Walk

Figure 2.4 shows 3 measures of performance on the BW (columns; Footfaults, partial falls, and Time to cross) against 4 impact and kinematic parameters (rows; Angular acceleration, linear acceleration, bolt target, and measured bolt throw). Number of footfaults (Figure 2.4 A, D, G, J) showed mixed correlation results, but did show a positive correlation that approached significance with bolt target (Figure 2.4 G; $R^2 = 0.3474$, $P = 0.0949$). Partial falls (Figure 2.4 B, E, H, K) also showed mixed correlation results, with target being the strongest factor (Figure 2.4 H; $R^2 = 0.3175$, $P = 0.1141$). Time to cross (Figure 2.4 C, F, I, L) also showed no clear trends, with no correlations approaching significance.

Inverted Wire Mesh

Hanging time on the IWM task was compared with impact measures (Figure 2.5). Kinematic parameters angular acceleration (A) and linear acceleration (B) showed negative correlation and linear acceleration approached significance ($R^2 = 0.447$, $P = 0.0697$).

Open Field

Similarly, delta compared to pre TBI of time spent in the center of the OF arena (A, C, E, G) and delta distance traveled (B, D, F, H) against angular acceleration, linear acceleration, bolt target, and measured bolt throw showed mixed relationships. Only delta time in the center zone against linear acceleration (C) approached significance ($R^2 = 0.3462$, $P = 0.5689$) and none of the impact variables approached significance for delta distance traveled.

2.5 Discussion

In this chapter we introduce a method for kinematic analysis of FRCHTBI models using high speed video capture and open source point tracking software. We further demonstrate applications of the method for quantifying injury consistency within cohorts and comparing injury properties to performance on behavioral testing.

Kinematic Properties of Impacts Varied, Even Under The Same Conditions

Even within a group of impacts with the same input settings, there was variation in both measured values of impact settings that were intended to be the same and kinematic properties of the injury (Figure 2.3). Bolt target (Figure 2.3 C) and bolt throw (Figure 2.3 D) likely varied impact to impact due to the speed at which animals needed to be transported from the anesthetic induction chamber to the impact platform to ensure the light plane of anesthesia was maintained at the time of impact. The bolt throw was also set using a sham animal each day before TBI was administered, and slight differences in the animal sizes might contribute to further variation. Future FRCHTBI models may attempt to mitigate some of these issues by incorporating placement guides for the animals head into the apparatus. It is important, however, that these do not interfere with the visibility of tracked points for filming or the free movement of the animals head upon impact. Angular and linear acceleration also varied within these impacts (Figure 2.3 A and B). This variation could be explained by the human error introduced with animal placement as well as slight variations in foil platform breakaway resistance and breakaway depth (which could change the point of the animals body that acts as the fulcrum for rotation during the post impact flip).

Specific Deficits May be Predicted by Specific Kinematic Properties

Variation in setting and kinematic properties of impacts, once captured, can be used to explore which factors contribute to different measured deficits. Even within the range of variation produced by impacts of 450g from 135cm with 3cm throw, trends emerged suggesting specific types of deficits may be influenced more by different properties. Post TBI deficits in coordination, measure by the BW, correlated most strongly with bolt targeting (Figure 2.4), possibly indicating a specific range of targeting is most likely cause damage within the primary or secondary motor cortical areas. In contrast, deficits in grip strength on the IWM (Figure 2.5) and changes in anxiety-like behavior in the OF (Figure 2.6) were most strongly correlated with kinematic properties of the injury, specifically linear acceleration. Expanding this method to include mild, moderate, and severe outcomes could elucidate

relationships between injury and kinematic parameters.

2.6 Conclusion

This method allows researchers to capture variance in injury settings and kinematic properties of FRCHTBI models and include these data in outcome analysis. In the present study we compared these measurements from a single cohort of impacts (450g from 135 cm with 3 cm throw) to outcomes in short term behavioral tasks from pre and 30 min post impact. However, the method could easily be applied to deficits measured by longer term behavior testing or even to help determine factors contributing to results of biochemical assays. It may also prove useful in providing the field of TBI research field with more clearly defined guidelines for what properties of mild, moderate, or severe impacts are that do not rely entirely on the outcomes for definitions and help with injury optimization between groups with different FRCHTBI induction apparatuses (or even nominally similar apparatuses with small differences that may affect injury induction).

2.7 Figures

Impact Settings (Drop Weight, Drop Height, Bolt Throw)	Rat Weight (g)	Bolt Throw (cm)	Bolt Target (cm)	Linear Velocity (m/s)	Linear Acceleration (m/s ²)	Angular Velocity (rad/s)	Angular Acceleration (rad/s ²)
305 g, 135 cm, 3 cm (n = 3)	487.33 ± 4.04	2.97 ± 0.08	1.7 ± 0.19	5.61 ± 0.27	544.14 ± 47.63	296.94 ± 52.94	33,408.18 ± 6,858.91
450 g, 135 cm, 3 cm (n = 18)	295.78 ± 110.15	2.42 ± 0.49	1.64 ± 0.19	5.38 ± 0.38	533.99 ± 41.68	283.94 ± 114.22	33,596.16 ± 12,270.53
450 g, 135 cm, 4 cm (n = 3)	477.67 ± 49.81	4.25 ± 0.48	1.48 ± 0.34	5.43 ± 0.08	518.24 ± 26.66	265.74 ± 86.61	31,004.42 ± 11,642.14
610 g, 67.5 cm, 1 cm (n = 3)	504 ± 17.32	1.56 ± 0.15	1.57 ± 0.12	4.29 ± 0.39	415.39 ± 44.07	316.99 ± 109.6	36,725.01 ± 12,846.27
610 g, 67.5 cm, 3 cm (n = 2)	504 ± 59.4	3.38 ± 0.39	1.34 ± 0.22	3.8 ± 0.33	380.72 ± 51.92	315.14 ± 26.95	36,288.77 ± 3,216.76
610 g, 135 cm, 1 cm (n = 3)	506.67 ± 23.09	1.27 ± 0.06	1.57 ± 0.2	4.75 ± 0.34	491.26 ± 36.19	271.75 ± 17.7	31,618.73 ± 2,192.54
610 g, 135 cm, 3 cm (n = 4)	455 ± 18.71	3.43 ± 0.29	1.57 ± 0.35	5.45 ± 0.65	535.77 ± 57.02	239.99 ± 54.03	27,736.81 ± 6,261.28
610 g, 135 cm, 4 cm (n = 3)	472 ± 26.29	4.26 ± 0.13	1.27 ± 0.28	5.57 ± 0.7	550.93 ± 64.72	295.59 ± 79.7	32,205.27 ± 11,004.05

Table 2.1: Kinematic measurements and injury properties with varied injury input parameters.

Peak values for linear and angular velocity and acceleration varying impact parameters for the TBI apparatus: drop weight (305, 450, and 610 g), drop height (67.5, 135 cm), and intended bolt throw (1, 3, 4cm)

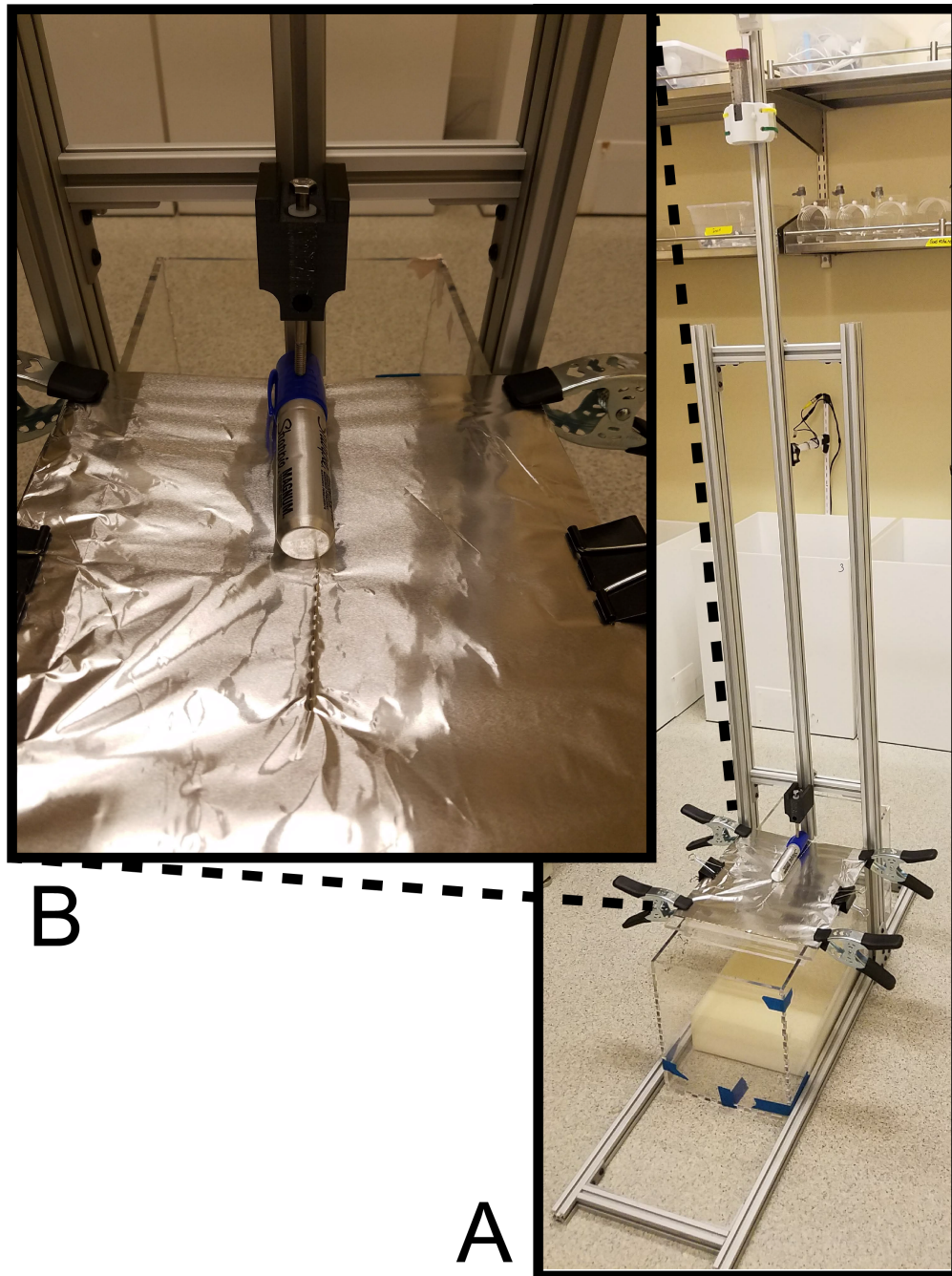


Figure 2.1: Drop-weight bolt-transfer FRCHTBI apparatus with inlay of breakaway platform
(A) Bolt transfer FRCHTBI apparatus used for impacts. (B) Close up of breakaway foil platform with modification to decrease variation in platform tension and breakaway consistency.

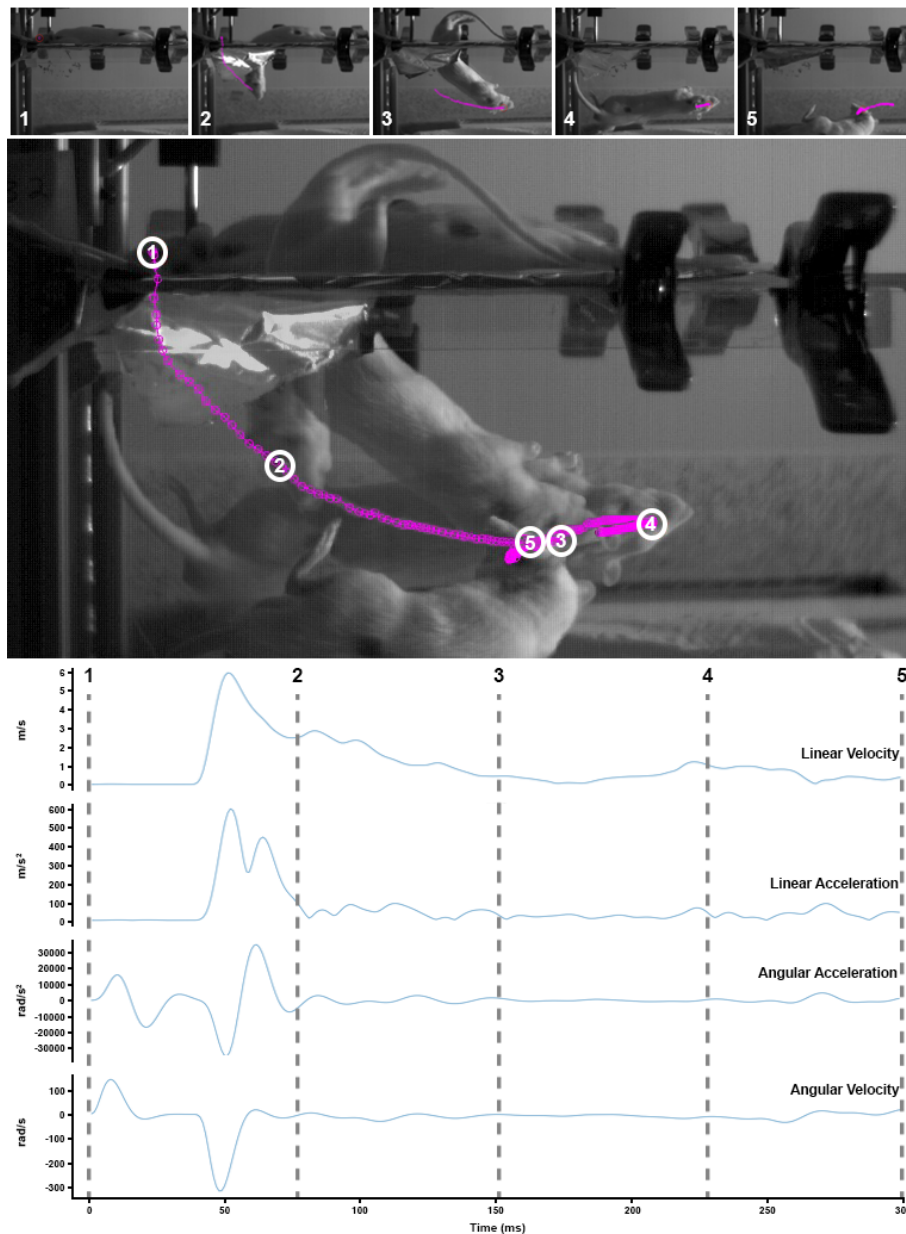


Figure 2.2: Point tracking and kinematic traces of a representative impact Top panel: Point tracking for 5 segments 500 ms with 450 g, 135 cm, 3 cm impact settings spanning immediately pre-impact (1) to just before coming to rest (5). Middle panel: A composite of the complete tracking path with the rats position at each of the frames from the top panel visible and labeled. Bottom panel: Frame by frame values for instantaneous linear and angular velocity and acceleration. Dashed lines are labeled with the representative time points from frames 1 - 5 in the top panel.

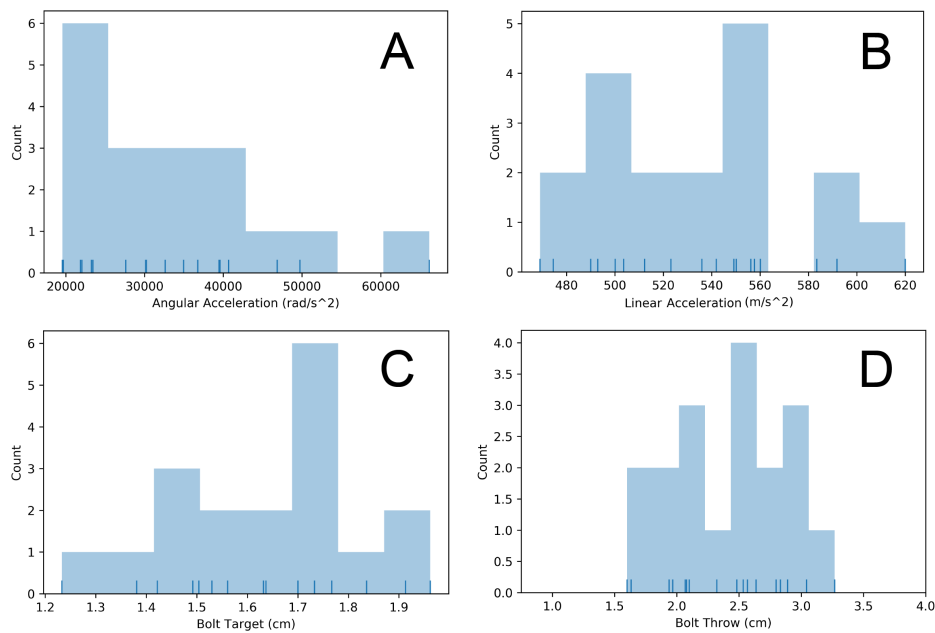


Figure 2.3: Distribution of kinematic measurements and impact properties for 450g, 135cm, 3cm.

Distribution of angular acceleration (A), linear acceleration (B), bolt target (C), and measured bolt throw (D) from TBI impacts from the 450 g from 135 cm with 3 cm bolt throw group ($n = 18$).

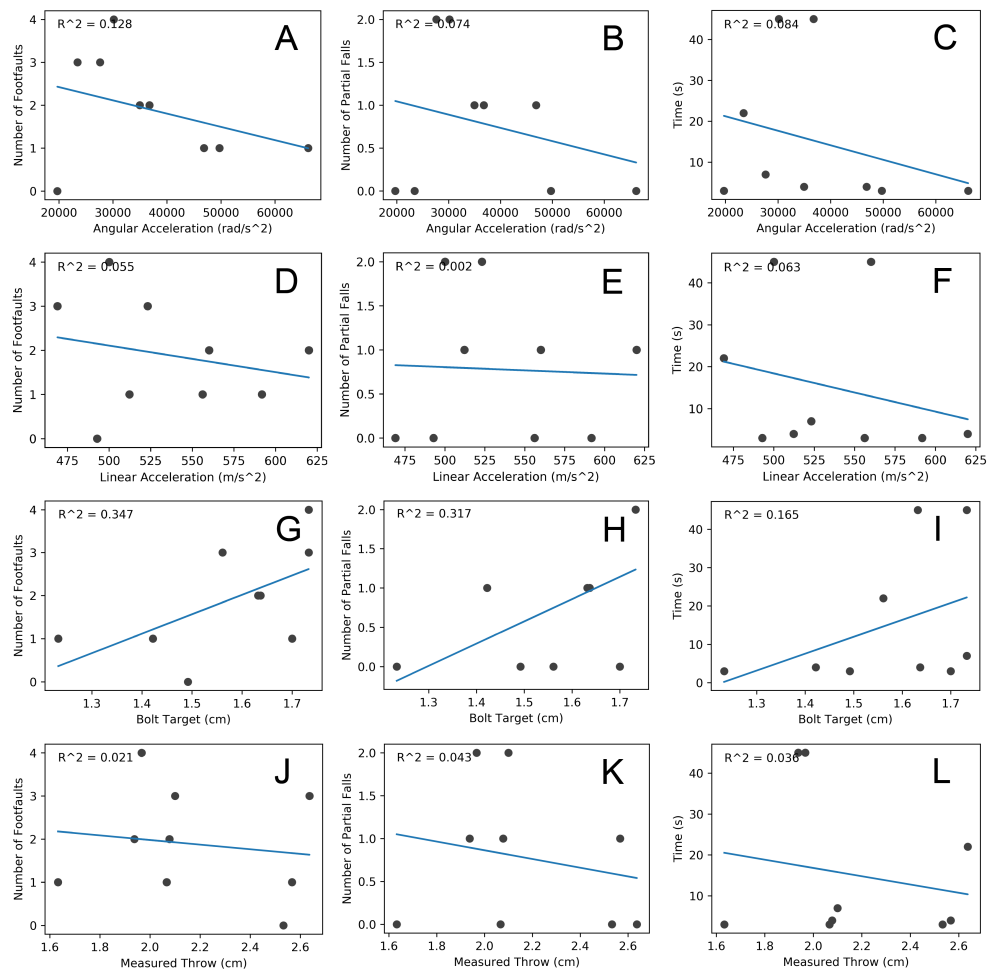


Figure 2.4: Impact properties and beam-walk performance.

BW performance metrics (columns; Footfaults, partial falls, and Time to cross) against impact and kinematic parameters (rows; Angular acceleration, linear acceleration, bolt target, and measured bolt throw). Footfaults against bolt target (G) approached significance ($P = 0.0949$).

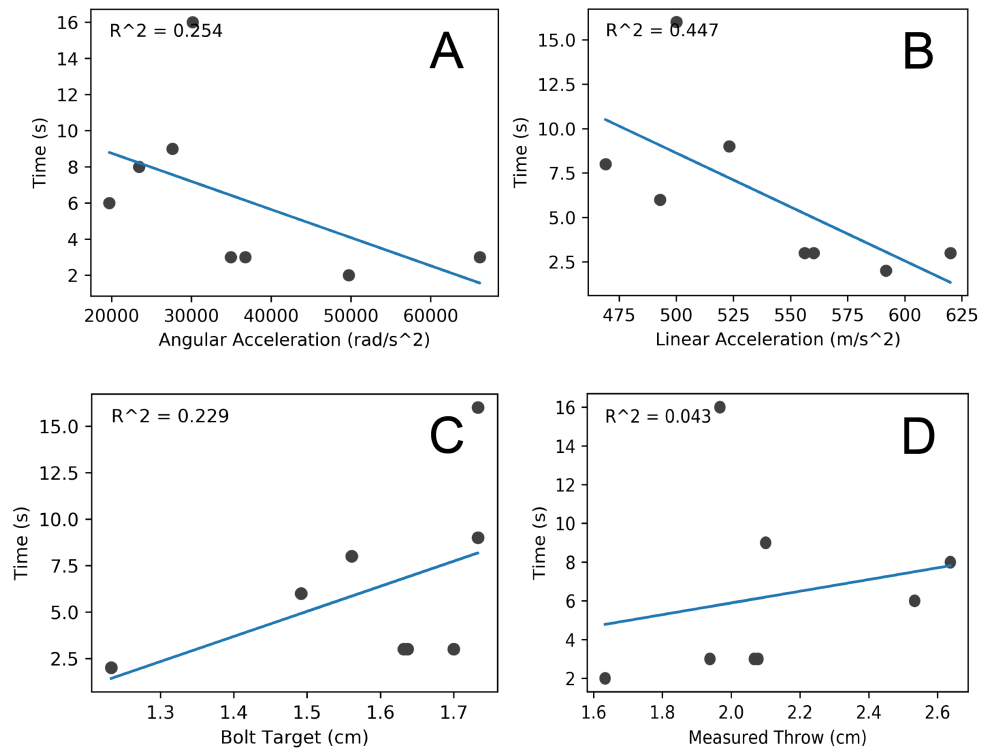


Figure 2.5: Impact properties and inverted wire mesh performance.

Inverted wire mesh hang time against kinematic parameters angular acceleration (A) and linear acceleration (B) and impact properties bolt target (C) and measured bolt throw (D).

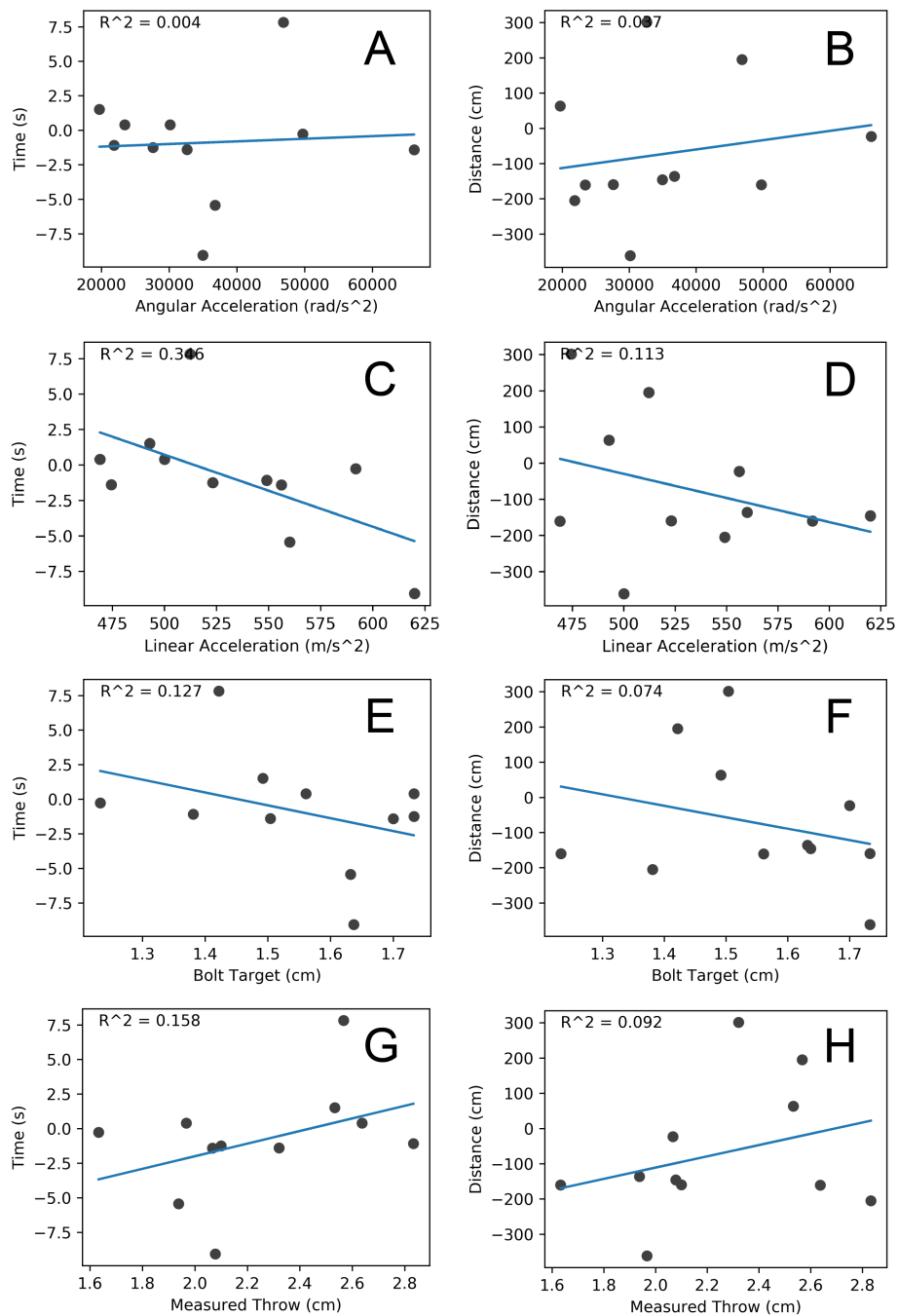


Figure 2.6: Impact properties and delta time in center of arena and delta distance traveled for open field.

Delta pre to 30 min post TBI of time spent in the center of the OF arena (A, C, E, G) and delta distance traveled (B, D, F, H) against angular acceleration, linear acceleration, bolt target, and measured bolt throw.

Chapter 3

Light Aversion and Gait Analysis as Low Cost, Clinically Relevant Assays for Murine TBI Evaluation

3.1 Abstract

Even simple pieces of equipment designed and marketed for scientific use (acrylic open field boxes, for example) are typically sold at incredible markups over cost of material and assembly, and all in one hardware and software solutions from commercial suppliers often involve immense license fees. This can be prohibitive for labs studying deficits in TBI models, and can lead to labs using the tests they have equipment for instead of ones that may be most relevant or sensitive. Our aim was to establish a pair of rodent behavioral assays that: 1. Effectively measure outcomes relevant to clinical TBI assessment and outcomes (namely photosensitivity and changes in gait patterns), 2. Require few pieces of specialized equipment and can be easily constructed from readily available and cheaply attainable components, and 3. Can be easily adapted by labs into their existing assessment and outcome testing for TBI studies. The modified LAV was able to detect differences in photosensitivity between sham and mTBI at 14 days post impact, and met all criteria for accessibility and ease of implementation. Gait analysis was able to detect changes in temporal (stance phase and swing phase) and spatial (step length) parameters 30 min post mTBI, although a high speed camera with fixed focus is required for best results (especially with available purpose specific software). However, we were able to extract results from videos (albeit with considerable extra effort) using a 240 fps recording mode on a camera phone under less than ideal circumstances.

3.2 Introduction

Sensory sensitivities are commonly presented as symptoms following TBI and photosensitivity has been reported in TBI in the weeks and month following mild injury (Waddell and Gronwall, 1984; Dikmen et al., 2010), with symptoms in some cases persisting 6 months to a year or beyond (Bohnen et al., 1991; Dikmen et al., 2010). Furthermore, persisting post TBI photosensitivity has been linked to aspects of chronic disability, sleep disturbances, post traumatic stress disorder (PTSD), and health-related quality of life measures (Callahan and Lim, 2018; Elliott et al., 2018; Shepherd et al., 2020). Despite the well documented inclusion of photosensitivity as a common and often sustained symptom of TBI, well defined interventions are not established (Callahan and Lim, 2018). While much of the data for human photosensitivity is self reported, this is not an option with animal models where much of the early evaluation of the efficacy of treatments on outcomes is tested. Therefore, a reliable assay for assessment of photosensitivity in rodent TBI would improve understanding of this common side effect and help elucidate efficacy of potential treatments.

In addition to sensory sensitivity, vestibular dysfunction is a common affliction following TBI (Arshad et al., 2017; Marcus et al., 2019). This can be assessed by evaluating for abnormalities in spatial, temporal, and kinematic properties of walking (Williams et al., 2009) and running gait (Williams et al., 2013), as well as balance (Row et al., 2019). Increasingly, efficacy of pairing gait assessment with cognitive challenges via dual or multi-task testing have shown promise over standalone gait analysis (Fino et al., 2018). While physical therapy regimens for addressing balance and coordination deficits have been established and may show promise and are recommended by some researchers (Basford et al., 2003; Ustinova et al., 2015), their broader outcomes have not been sufficiently documented in the literature (Bland et al., 2011). For these reasons, it is clinically valuable to include measures of changes in gait parameters for experimental TBI models to detect presence and severity of motor and vestibular deficits, as well as efficacy of treatment.

Even simple pieces of equipment designed and marketed for scientific use (acrylic open field boxes, for example) are typically sold at incredible markups over cost of material and assembly, and all in one hardware and software solutions from commercial suppliers often involve immense license fees. This can be prohibitive for labs measuring deficits in TBI models, and can lead to labs using the tests they have equipment for instead of ones that may be most sensitive or relevant.

Here, I aim to establish a pair of rodent behavioral assays that: 1. Effectively measure outcomes relevant to clinical TBI assessment and outcomes (namely photosensitivity and changes in gait patterns), 2. Require few pieces of specialized equipment and can be easily constructed from readily available and cheaply attainable components, and 3. Can be easily adapted by labs into their existing assessment and outcome testing for TBI studies. To the best of our knowledge, this is the first use of a LAV assay without a clear sided light

compartment (as with the traditional light/dark box assay, designed to measure anxiety and not photosensitivity) in murine models of TBI evaluation.

3.3 Methods

Animals

All animal procedures were approved by the ACUC at the University of California Berkeley. Male Sprague Dawley rats were purchased from Charles River USA (Wilmington, MA) at 49 days of age and individually housed. Animals were tested 25 days after arrival to reproduce the time line of the associated study the assay was being optimized for. Cages were maintained at a constant temperature and humidity with a 12 hour light-dark cycle (light 7:00 am to 7:00 pm) and animals were given unrestricted access to water and chow. FRCHTBI induction used the same FRCHTBI method and apparatus described in chapter 2, dropping 450g from 135 cm with 3 cm of bolt throw.

Light Aversion Assay

Arena

The LAV arena and procedure were modified for use with rats from Thiels et al. (2008). An OF arena constructed of opaque acrylic measuring 50 x 50 X 60 cm (L x W x H) was fitted with a black acrylic insert bisecting the arena to create two 50 x 25 x 60 cm compartments. Unhindered access to both compartments was provided via a 10 x 10 cm opening in the center of the insert separating the compartments. The top of each compartment was covered with either a black (dark compartment) or clear acrylic lid (light compartment). Light intensity in the light compartment was controlled by a 300W slide control dimmer with 17.5 LED dimmable bulbs with 1,600 lumen max and 3,000K warmth rating (Feit Electric; Pica Rivera, CA) shining directly through the lid. Trials were recorded through the clear acrylic lid on a Logitech C270 Webcam (Logitech International; Newark, CA) such that the base of all light compartment walls and the opening of the insert were clearly visible. All acrylic was purchased from Tap Plastics, Inc. (San Leandro, CA).

Procedure

Tests were conducted in a quiet behavior room with red overhead lighting. Rats were dark adapted by placing their home cage in a covered holding arena for 60 min prior to assay administration. Prior to each trial the desired light intensity (lux) was achieved by adjusting the dimmer and confirming with a luxmeter and readings in the dark compartment were confirmed to be <5 lux under all conditions. Each test consisted of 4 trials with increasing light intensities. Rats were placed in the dark compartment of the arena, and left undisturbed for 5 minutes from the time the lid was replaced. After 5 minutes (or as

soon after as the animal returned to the dark compartment), animals were returned to their home cage in the holding arena for 5 minutes before starting beginning the next trial. This procedure was repeated for all trials. After the final trial all arena surfaces, including walls and partitions, were cleaned with and thoroughly dried in sequence with 1. Formula 409 Multisurface Cleaner (The Clorox Company; Oakland, CA), 2. 1% acetic acid, and 3. .004% NPD to prepare for the next rat.

Initial observed trials ($n = 3$, data not reported) used a sequence of 0, 500, 1,000, and 1,500 lux. Because these settings were deemed to be too bright to see a graded difference in wild type rats, a second round of observed trials ($n = 3$, data not reported) were run with 0, 250, 500, and 750 lux. Final optimization trials ($n = 6$) and TBI testing validation trials (Sham $n = 6$, TBI $n = 6$) used a sequence of 0, 250, 500, and 750 lux. In order to control for time of day effects and any slight variations in environmental conditions that might have arisen two arenas were built and the LAV was administered to one animal from each group simultaneously alternating group arena assignments.

LAV Scoring

The first 5 minutes of each trial was scored by 2 individuals blinded to the condition of the video and scores were reported as the average. If the coefficient of variance (CV) for any measure was greater than 10% the video was reviewed by a third individual to determine the source of discrepancy. Frequency and latency to first occurrence of the head, front limbs, and all limbs crossing from the dark to light compartments was recorded. Cumulative time in the light compartment with front limbs (inclusive of all limbs) and all four limbs was recorded and subtracted from 300 s to determine time in the dark compartment for each. For time in light measures, recorded time stopped as soon as the rats head or referenced limbs crossed from the light to dark compartment (whichever occurred first).

Gait Analysis

Gait Walkway

The LAV arena and procedure were based on a previously published gait analysis system, Mousewalker (Mendes et al., 2015) built from readily available components with modifications for use with rats. Briefly, a 6 x 48 inch platform of 1/4 inch clear acrylic was lined along the length with color LED strip lights held in place by aluminum U channels and lined with weather stripping to direct all light directly into the platform. A clear acrylic wall was built to fit over the platform (12 x 6 x 48 inches, h,w,l) to contain the rats during trials. An acrylic mirror (7 x 48 in) was placed below the platform at a 45 degree angle to reflect light captured underneath the platform for filming. It is worth noting that the structural components holding the platform from the MouseWalker build did not scale to the rat sized apparatus, and we instead rested the platform on a set of adjustable shelves that accommo-

date clearance of the mirror underneath. While this has the advantage of being modular and quickly breaking down to compactly stored components, for those with limited behavioral space, the build detailed by Jacobs et al. (2018) is highly recommended as an alternative for those with the storage capacity.

Procedure

One day before TBI animals were acclimatized to the gait walkway by allowing them to explore for 2 minutes under the same lighting settings as recorded trials. Trials included in analysis were filmed within an hour before impact and 30 min post impact with red LED lighting for the walkway and dim red overhead lighting in the room. Rats were given two minutes to freely explore, and if they had not produced at least two passes from one end of the platform to the other without stopping they were placed in a corner and gently prodded to encourage crossing. Videos were filmed on a Samsung Galaxy S7 Edge (Samsung; San Jose, CA) using the slow motion capture at a frame rate of 240 fps. It is worth noting that this led to a higher than acceptable amount of variability in video quality and a single purpose slow motion capture video camera is recommended for gait analysis, and will be used in future trials.

Video Processing

Full videos were clipped into single passes that spanned at least 75% of the distance of the walkway without interruption (stopping, rearing, turning around, etc.). The open source software LosslessCut (github.com/mifi/lossless-cut), a graphical user interface built on FFmpeg (ffmpeg.org), was used for this step to insure there was no quality loss or decrease in frame rate. After videos were cut into single pass clips these were cropped to include only the reflection of the walkway in the mirror using a script built in Matlab R2019a (mathworks.com). The two most complete passes for each animal at each time point were selected for further processing.

Deep Neural Network Based Point Tracking with DeepLabCut (DLC)

Processed (clipped and cropped) videos were used to train a deep neural network to track relevant points using DLC V2.2 (Mathis et al., 2018) as a multi-animal project. Fifteen frames were extracted and labeled from each video, making sure that each body part was able to be labeled at least twice. Corners of the gait platform were labeled and tracked to use as distance references during analysis. For the animal nose and tail-base were labeled in all frames and each paw was labeled when it was visibly in contact with the gait platform. All tracked points for the arena and animal were connected to each other point of that object using the skeleton settings to improve tracking performance. Each video was trained and analyzed on its own network trained with 50,000 iterations. This approach is not typical of the DLC process, as a major strength is the ability to label novel videos after training on a

subset, but gave better results given the variability of our videos and the added difficulty of tracking points that were only labeled intermittently.

Gait Parameter Extraction

The DLC from analyzed videos includes frame by frame x and y pixel values for each tracked part labeled in that frame, as well as likelihood values indicating the level of certainty each label is correct. From this information we extracted several paw by paw temporal (stance duration and stride time) and spatial (stride length and stride width) parameters for each stride.

To reduce the number of mislabeled points we first apply a filter based on likelihood values to only include labels with a very high level of certainty. For the videos analyzed in the present study including labels with > 0.9999 certainty tended to effectively reduce errant labels without removing correctly labeled parts. This filtered data set was used to determine the groups of frames where each paw was down, which was the basis of extracting the stance phases for each paw where the start frame and end frame were used to calculate stance duration and the average X and Y pixel values gave a single point from which to calculate spatial gate parameters. These recorded values from sequential stance phases were used to calculate stride length (linear distance between paired X and Y positions), stride width (distance between parallel lines of the rear right and left or front right and left paws from a stance phase), and stride time (end frame of one stance phase to start frame of the next). Finally, real world values were attributed by scaling temporal measurements from frames to ms (where 1 frame is equal to $1/240$ s) and spatial measurements from pixels to mm (using the known distance between corners to calibrate distance per pixel for each video).

Gait TBI Detection

Sham ($n = 3$) and TBI ($n = 3$) animals had gait walkway trails recorded less than an hour prior to and 30 min following a mTBI impact or sham injury (anesthetic procedure without a weight drop). From each trail, two crossings of the walkway that matched our criteria were selected for analysis and used to calculate stance phase, swing phase, and step length for each paw.

Statistical Analysis

Statistical analysis was performed using python module statsmodels v0.12.1 (Seabold and Perktold, 2010) in python v3.7.7 (Python Software Foundation, <https://www.python.org/>). Values were reported as mean \pm SD.

Light Aversion Assay

For LAV a one way Analysis of Variance (ANOVA) was run for each group to test for differences between lux settings for each measured variable. Post-hoc analysis was performed using Holm-dk pairwise multiple comparisons testing. P-values were reported after adjusting for multiple comparisons and were considered significant with $\alpha < .05$ and approaching significance with $\alpha < 0.1$.

Gait Analysis

Pre and post injury parameters were compared using pairwise t-tests for each paw pre vs post impact. P-values were reported after adjusting for multiple comparisons and were considered significant with $\alpha < .05$ and approaching significance with $\alpha < 0.1$.

3.4 Results

Light Aversion Assay Optimization

Light Intensity Optimization

An initial round of optimization trials using control rats was observed, but not scored. The first set of trials ($n = 3$) had a sequence of 0, 500, 1,000, and 1,500 lux and showed near complete dark preference in the 1,000 and 1,500 lux. A second observation only trial was run ($n = 3$) with a sequence of 0, 250, 500 and 750 lux. The animals in this second group showed a clear drop in time spent in light compartment between 0 and 250 lux, no apparent difference between 250 and 500 lux, and a clear but not complete preference for the dark compartment at 750 lux.

Trials with control rats and a sequence of 0, 250, 500, and 750 lux ($n = 6$) were recorded and scored to assess both the assay design and determine useful scoring measures (Figure 3.1). Neither latency to entering the light compartment with the front limbs (Figure 3.1 A) nor all limbs (Figure 3.1 B) were significantly different between trials (ANOVA $P = 0.4072$ and 0.4662 , respectively), although they were generally lowest at 0 lux and highest at 750 lux. Frequency of entries to the light compartment with the head (Figure 3.1 C) and front limbs (Figure 3.1 D) did not present any significant differences between trials (ANOVA $P = 0.2490$ and 0.2093 , respectively). Entries with all four limbs (Figure 3.1 D) showed significant differences between light intensities (ANOVA $P = 0.0094$) between 0 - 750 lux ($P = 0.0088$), and was approaching significance for 0 - 250 and 0 - 500 lux ($P = 0.075$ and 0.0595 , respectively). Time in the light compartment with front limbs (Figure 3.1 F) and all limbs (Figure 3.1 G) both showed differences between trials (ANOVA $P = 0.0096$ and $.0094$, respectively), and in both measures significance was detected between 0 - 750 lux ($P = 0.0066$ and 0.0088 , respectively). Comparisons between 0 - 250 and 0 - 500 lux approached significance for time in light with all limbs ($P = 0.0754$ and 0.0595 , respectively).

TBI Detection Validation

Based on results of the intensity optimization, a trial sequence of 0, 250, 500, and 750 lux was used to validate the ability of the assay to detect photosensitivity in mild TBI ($n = 6$) relative to sham injury ($n = 6$). Frequency of entry to the light compartment with the front limbs (Figure 3.2 A) was not significantly different between intensities for sham (ANOVA $P = 0.1153$), and approached significance for TBI (ANOVA $P = 0.0708$, 0 - 750 lux $P = 0.0909$). Frequency of entry to the light compartment with all limbs (Figure 3.2 B) was not significantly different between intensities for sham (ANOVA $P = 0.2817$), but showed significant differences for TBI for 0 - 750 lux ($P = 0.0116$) and approached significance for 0 - 500 lux ($P = 0.0944$). Time spent in the light compartment with front limbs (Figure 3.2 C) showed significant difference in sham animals at for 0 - 250 ($P = 0.04$), 0 - 500 ($P = 0.0268$), and 0 - 750 lux ($P = 0.0138$) and TBI animals for 0 - 250 ($P = 0.0437$), 0 - 500 ($P = 0.0116$), and 0 - 750 lux ($P = 0.0116$). Time spent in the light compartment with all limbs (Figure 3.2 C) for was significantly different for 0 - 750 lux ($P = 0.0195$) and approached significance for 0 - 250 ($P = 0.0716$) and 0 - 500 lux ($P = 0.0707$) in sham animals and TBI animals spent significantly less time in the light compartment at all intensities relative to 0 lux; 0 - 250 ($P = 0.0495$), 0 - 500 ($P = 0.0105$), and 0 - 750 lux ($P = 0.0105$).

Gait Analysis

Gait Parameter Extraction Pipeline

In order to ensure only reliable labels were used from the DLC output a filter for likelihood > 0.9999 was applied to the data. This tended to produce the accurate points without a large loss of correctly labeled frames. Figure 3.3 shows a representative labeling for all body parts before (A) and after (B) applying this filter. From this filtered data, paw placement and duty cycle information was extracted (Figure 3.4) and used to calculate temporal and spatial metrics for each paw for stance phase and stride measurements.

Spatial and Temporal Gait Parameters After TBI

Stance phase for all paws increased from pre to post injury in TBI animals, and in one paw for sham (Figure 3.5). Front right (Figure 3.5 A), front left (Figure 3.5 B), and rear right (Figure 3.5 C) paws increased average time of stance phase in TBI animals only ($P = 0.0002$, $P = 0.0022$, and $P = 0.0005$, respectively), while rear left (Figure 3.5 D) paw increased in both sham and TBI animals ($P = 0.0465$ and $P = 0.0011$, respectively).

Swing phase for all paws increased from pre to post injury in TBI animals (Figure 3.6). Front right (Figure 3.6 A), front left (Figure 3.6 B), rear right (Figure 3.6 C), and rear left (Figure 3.5 D) paws increased average swing phase in TBI animals ($P < 0.0001$, $P < 0.0001$, $P = 0.0013$, and $P < 0.0001$, respectively).

Step length for 3 paws decreased from pre to post injury in TBI animals (Figure 3.7). Front right (Figure 3.7 A), front left (Figure 3.7 B), and rear left (Figure 3.7 D) paws increased average step length in TBI animals ($P = 0.0068$, $P = 0.0076$, and $P = 0.0057$, respectively). Rear left (Figure 3.7 D) paw approached significance in sham ($P = 0.0957$) and rear right (Figure 3.7 C) approached significance in TBI ($P = 0.0659$).

3.5 Discussion

Light Aversion Assay Optimization

Light Intensity Optimization

An initial round of optimization trials using control rats was observed, but not scored. The first set of trials ($n = 3$) had a sequence of 0, 500, 1,000, and 1,500 lux and showed near complete dark preference in the 1,000 and 1,500 lux. A second observation only trial was run ($n = 3$) with a sequence of 0, 250, 500 and 750 lux. The animals in this second group showed a clear drop in time spent in light compartment between 0 and 250 lux, no apparent difference between 250 and 500 lux, and a clear but not complete preference for the dark compartment at 750 lux.

Trials with control rats and a sequence of 0, 250, 500, and 750 lux ($n = 6$) were recorded and scored to assess both the assay design and determine useful scoring measures. Neither latency to entering the light compartment with the front limbs (Figure 3.1 A) nor all limbs (Figure 3.1 B) were significantly different between trials (ANOVA $P = 0.4072$ and 0.4662 , respectively), although they were generally lowest at 0 lux and highest at 750 lux. Frequency of entries to the light compartment with the head (Figure 3.1 C) and front limbs (Figure 3.1 D) did not present any significant differences between trials (ANOVA $P = 0.2490$ and 0.2093 , respectively). Entries with all four limbs (Figure 3.1 D) showed significant differences between light intensities (ANOVA $P = 0.0094$) between 0 - 750 lux ($P = 0.0088$), and was approaching significance for 0 - 250 and 0 - 500 lux ($P = 0.075$ and 0.0595 , respectively). Time in the light compartment with front limbs (Figure 3.1 F) and all limbs (Figure 3.1 G) both showed differences between trials (ANOVA $P = 0.0096$ and $.0094$, respectively), and in both measures significance was detected between 0 - 750 lux ($P = 0.0066$ and 0.0088 , respectively). Comparisons between 0 - 250 and 0 - 500 lux approached significance for time in light with all limbs ($P = 0.0754$ and 0.0595 , respectively). Collectively, this sequence of intensities appeared to show a graded response in control animals with measures with potential for differentiation between small and large differences in light sensitivity (entries and time in light, in particular), showing potential for assessment across various severities of TBI.

TBI Detection Validation

Based on results of the intensity optimization, a trial sequence of 0, 250, 500, and 750 lux was used to validate the ability of the assay to detect photosensitivity in mild TBI ($n = 6$) relative to sham injury ($n = 6$). Frequency of entry to the light compartment with the front limbs (Figure 3.2 A) was not significantly different between intensities for sham (ANOVA $P = 0.1153$), and approached significance for TBI (ANOVA $P = 0.0708$, 0 - 750 lux $P = 0.0909$). Frequency of entry to the light compartment with all limbs (Figure 3.2 B) was not significantly different between intensities for sham (ANOVA $P = 0.2817$), but showed significant differences for TBI for 0 - 750 lux ($P = 0.0116$) and approached significance for 0 - 500 lux ($P = 0.0944$). Time spent in the light compartment with front limbs (Figure 3.2 C) showed significant difference in sham animals at for 0 - 250 ($P = 0.04$), 0 - 500 ($P = 0.0268$), and 0 - 750 lux ($P = 0.0138$) and TBI animals for 0 - 250 ($P = 0.0437$), 0 - 500 ($P = 0.0116$), and 0 - 750 lux ($P = 0.0116$). Time spent in the light compartment with all limbs (Figure 3.2 D) for was significantly different for 0 - 750 lux ($P = 0.0195$) and approached significance for 0 - 250 ($P = 0.0716$) and 0 - 500 lux ($P = 0.0707$) in sham animals. TBI animals spent significantly less time in the light compartment at all intensities relative to 0 lux; 0 - 250 ($P = 0.0495$), 0 - 500 ($P = 0.0105$), and 0 - 750 lux ($P = 0.0105$). Collectively these trials suggest the modification made to the LAV were able to detect small differences in photosensitivity between sham and animals with a mTBI. Measures of frequency and time spent in the light compartment with all limbs appear to discriminate better than lower commitment measurements using the head and front limbs.

Evaluation of Spatial and Temporal Gait Parameters with a Combination of Open Source Tools

Video Processing and Deep Neural Network Based Point Tracking with DLC

Due to the variation in video quality and changes from the gait walkway and recording setup, analysis with MouseWalker analysis software was unsuccessful at extracting gait parameters. For this reason, we created a pipeline of open source software for processing videos to prepare for point tracking in DLC (Mathis et al., 2018) and extracting gait parameters from the tracked output.

The selection of a tool for the video processing steps is critical, as it must not alter the frame quality or the playback rate of the resulting clips (many commonly available video clipping tools do not support 240 FPS output). We chose the open source software LosslessCut (github.com/mifi/lossless-cut), a useful graphical user interface built on FFmpeg (ffmpeg.org), that enables clipping videos without encoding and decoding, therefore maintaining native frame by frame and playback properties of the original video. In the present study we further processed the videos to include only the mirrored reflection of the gait walkway using Matlab, which requires a license. It is worth noting that open source alter-

natives exist and this step is not absolutely necessary as DLC allows for crop settings to be set internally as well.

DLC (Mathis et al., 2018) was chosen for point tracking of processed gait videos. DLC uses deep neural networks to learn how to label behavior videos based on minimal human input (in our case, labeling 15 frames per 400+ frame video). This robust training approach should typically be able to take frames from a small subset of videos and extrapolate this labeling accurately to other videos filmed under the same conditions. However, because this works more reliably when body parts are visible consistently (as opposed to the paws only being labeled when in contact with the platform) and our videos not proving to be consistent enough with regards to focus (and the resulting contrast between paws and the body from the walkway) we trained each video on its own network to achieve the most reliable labeling. Even so, it was a considerable time savings relative to manually tracking each video. In cases where a more permanent setup is used for filming, training a single network that could be used for multiple studies worth of the same behavior task would save even more time.

Temporal and Spatial Gait Parameters Detect Mild mTBI

Both temporal (stance phase and swing duration) and spatial (step length) parameters showed promise in detecting mTBI 30 min post impact. There was an overarching theme of increased time spent in stance phase (Figure 3.5) and swing phase (Figure 3.6), as well as shorter step length (Figure 3.7) for TBI animals post impact. Taken collectively, these would suggest a decrease in overall movement speed and an injury that did not show a unilateral effects on gait change, which makes sense given the mid-line point of impact (as opposed to many models with lateral impacts). The directions of these trends corroborate with other analysis of gait following TBI, even if the magnitude of change was lower (Neumann et al., 2009). This supports the sensitivity of changes in even simple gait parameters in detecting TBI of multiple levels of severity, including mild.

Commercial and Open Source Alternatives for Gait Analysis

Admittedly, none of the gait measurements presented in the present chapter were novel in their application to TBI evaluation and several commercially available integrated hardware and software platforms are available for gait analysis, such as TreadScan (Clever Sys Inc.; Reston, VA) and CatWalk XT (Noldus; Leesburg, VA). For labs with access to these systems, they will likely produce more robust data in a more streamlined fashion. However, the aim of the current assay was to make available a lower commitment option for cases where these systems are cost prohibitive.

As alternatives, at least two open source platforms designed specifically for rodent gait analysis exist. Mousewalker (Mendes et al., 2015) and GAITOR (Jacobs et al., 2018). In our hands, MouseWalker did not work well with modifications of the videos made necessary

by changes to the gait apparatus when scaled for rats. The announcement publication for GAITOR was not available at the time of experimental design and early rounds of data collection. The gait apparatus was based on similar design and concepts, and it allows for synchronized capture and analysis of ventral and lateral views of the animal. This, along with the more application specific focus of the software would have likely made it a better choice and future TBI cohorts will likely utilize the GAITOR walkway and software.

Despite these gait specific open source alternatives that have become available, the current work presents an open source framework that can be applied to any behavior task for which there is no task specific analysis software, or for cases where videos do not meet quality or consistency standards for reliable results. Although it required training a network for each video, DLC was powerful enough in this application to allow extraction of relevant gait parameters from videos that purpose built software were not.

3.6 Conclusion

The work presented in this chapter aimed to establish a pair of rodent behavioral assays that measure outcomes relevant to human TBI, are low cost and easily constructed, require little specialized equipment, and can be easily integrated with existing TBI experimental work flows. LAV was able to detect differences in photosensitivity between sham and TBI 14 days post impact and met all criteria for ease of implementation. Gait analysis was able to detect differences in both temporal (stance phase and swing phase) and spatial (step length) parameters following mTBI as well. Our pipeline for gait video analysis was able to extract simple gait parameters, however with some added difficulty without a reliable filming setup. In this regard, the gait analysis does seem to require a high speed camera well suited for this purpose. Even with this critical piece of equipment, the available tools for analysis (either the open source pipeline used here or a purpose-built open source software such as GAITOR) allow labs a lower entry point for adding gait analysis as a meaningful part of their TBI assessment work flow compared to commercially available setups.

3.7 Figures

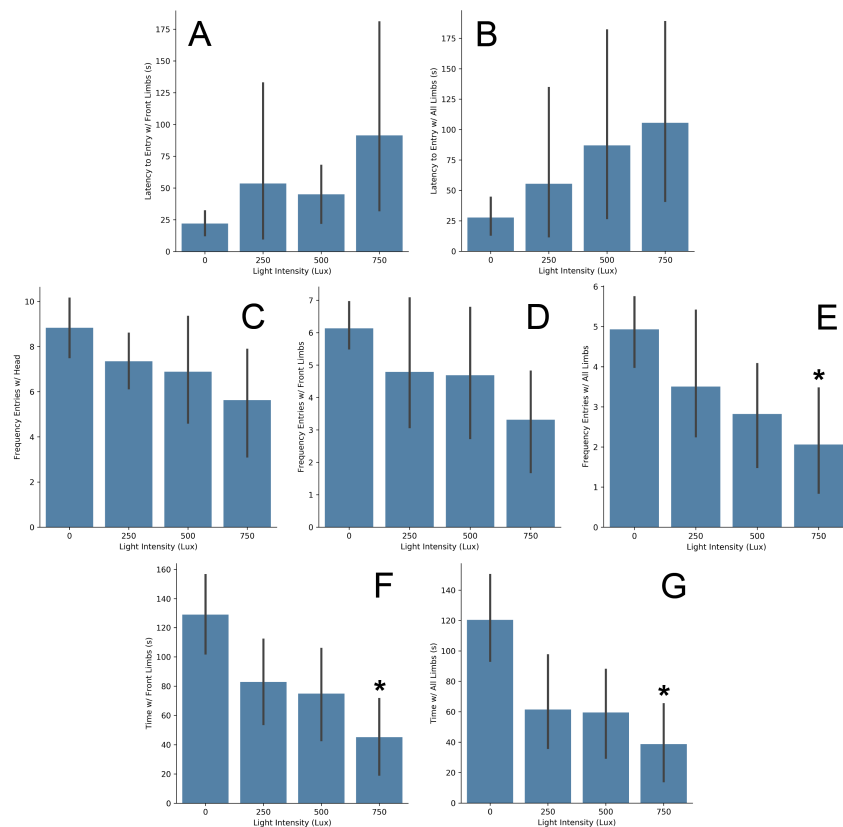


Figure 3.1: Light aversion assay optimization

Optimization cohort ($n = 6$) testing a intensity sequence of 0, 250, 500, and 750 lux based on previous observations. Latency to enter the light compartment with front limbs (A) and all limbs (B) did not show significant difference between any time points. Frequency of entries to the light compartment with the head (C) and front limbs (D) did not show significance between any time points. Frequency with all limbs (E) was significantly lower at 750 vs 0 lux ($P = 0.0088$) and approached significance for 250 vs 0 lux ($P = 0.075$) and 500 vs 0 lux ($P = 0.0595$). Time in the light compartment with front limbs (F) and all limbs (G) showed differences for 0 vs 750 lux ($P = 0.0066$ and 0.0088 , respectively) and approached significance with all limbs for 0 vs 250 and 0 vs 500 lux ($P = 0.0754$ and 0.0595 , respectively). * significant at $P < 0.5$ compared to 0 lux

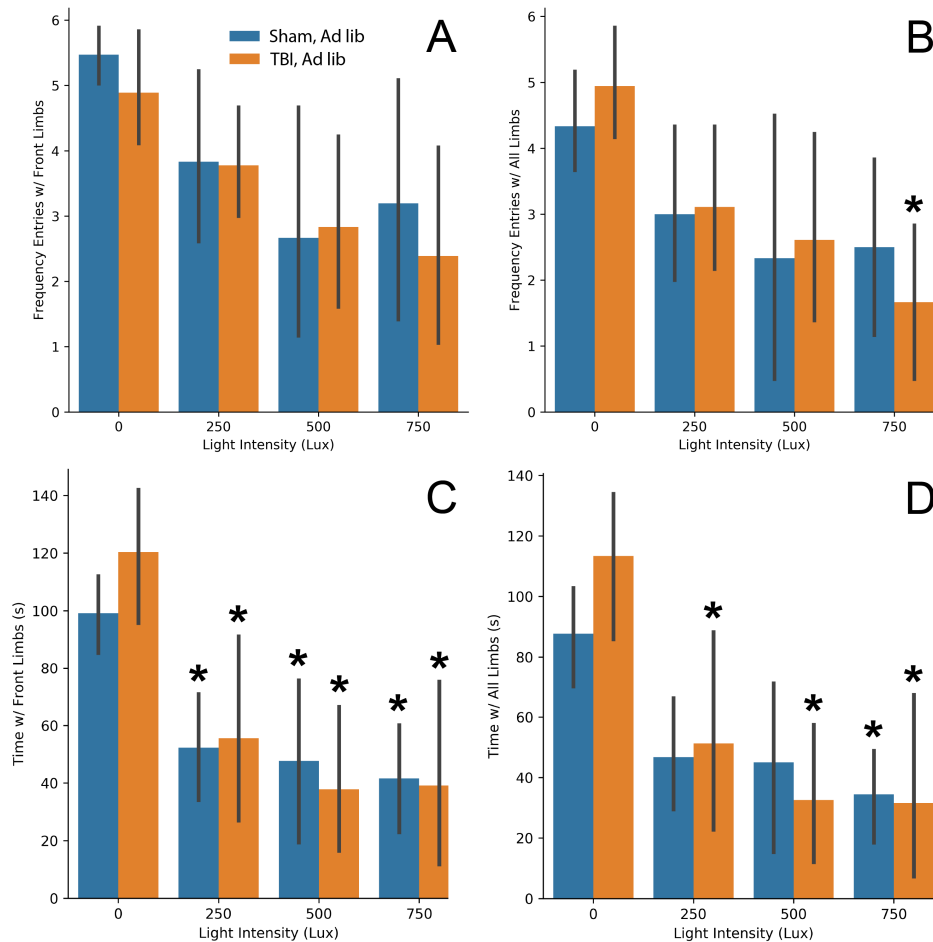


Figure 3.2: Light aversion assay TBI detection validation

LAV validation for detection of photosensitivity in TBI ($n = 6$) vs sham ($n = 6$) rats. Frequency of light compartment entries with front limbs (A) approached significance for 750 vs 0 lux in TBI ($P = 0.0909$). Frequency of entries with all limbs (B) was significant for 0 vs 750 lux in TBI ($P = 0.0116$) and approached significance for 0 vs 500 in TBI ($P = 0.0944$). Time spent in the light compartment with front limbs (C) was significantly different for 0 vs 250, 0 vs 500, and 0 vs 750 for sham ($P = 0.04$, $P = 0.0268$, and $P = 0.0138$, respectively) and 0 vs 250, 0 vs 500, and 0 vs 750 in TBI ($P = 0.437$, $P = 0.116$, and $P = 0.116$, respectively). Time spent in the light compartment with all limbs (D) was significant for 0 vs 750 ($P = 0.0195$), approached significance for 0 vs 250 and 0 vs 500 ($P = 0.0716$ and $P = 0.0707$, respectively) in sham, and was significant for 0 vs 250, 0 vs 500, and 0 vs 750 in TBI ($P = 0.0495$, $P = 0.0105$, and $P = 0.0105$, respectively).

* significant at $P < 0.5$ compared to 0 lux

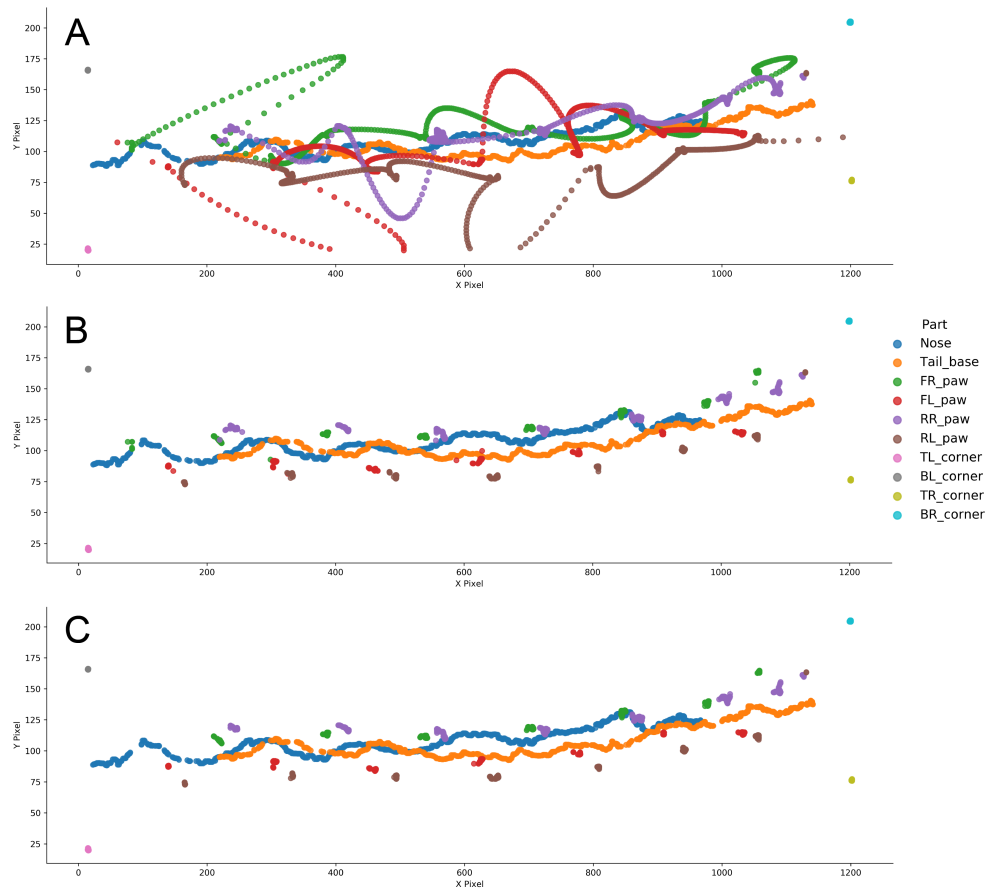


Figure 3.3: Likelihood filtering improves accuracy of tracked body part data
 Raw frame by frame position data for each body part from DLC can be filtered to improve the body part attribution and pixel location accuracy for calculating. Plots showing an example of raw labels plotted with frame by frame pixel values for a single pass from right to left on the walkway (A) and the same data after filtering for DLC likelihood probabilities of > 0.5 (B) and > 0.9999 (C). Corners of the walkway are labeled in each frame as reference (T = top, B = bottom, L = left, R = right) as well as 6 points on the rat (FR = front right, FL = front left, RR = rear right, RL = rear left). Paws are only labeled when visibly touching the walkway.

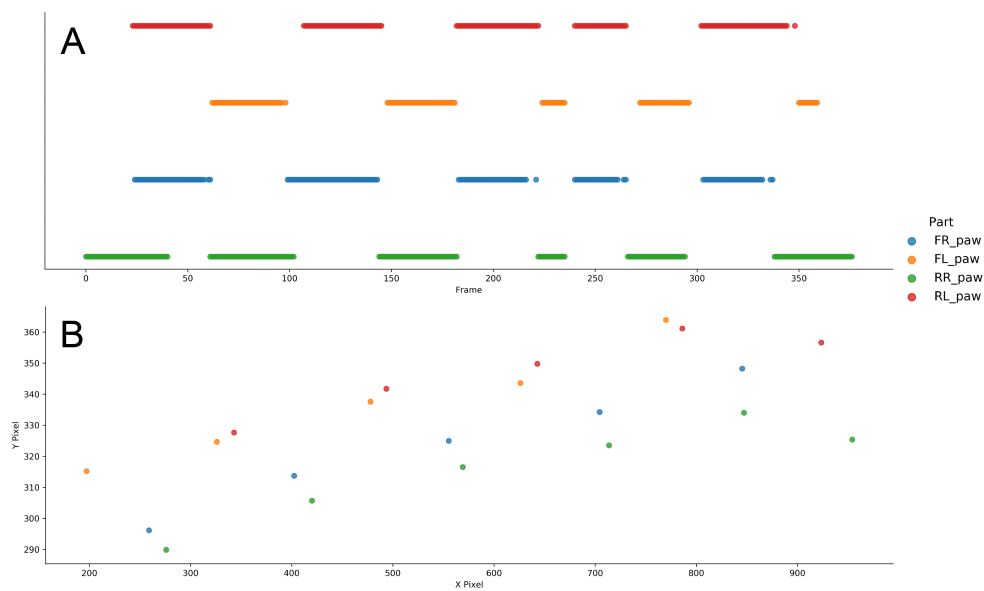


Figure 3.4: Temporal and spatial representation of stance phases from a single pass
Filtered paw labels from each frame can be plotted to present temporal properties of stance phases for each limb (A) and plotted as x and y pixel values per stance phase to visualize spatial distribution of stance phases for each limb (B). (FR = front right, FL = front left, RR = rear right, RL = rear left)

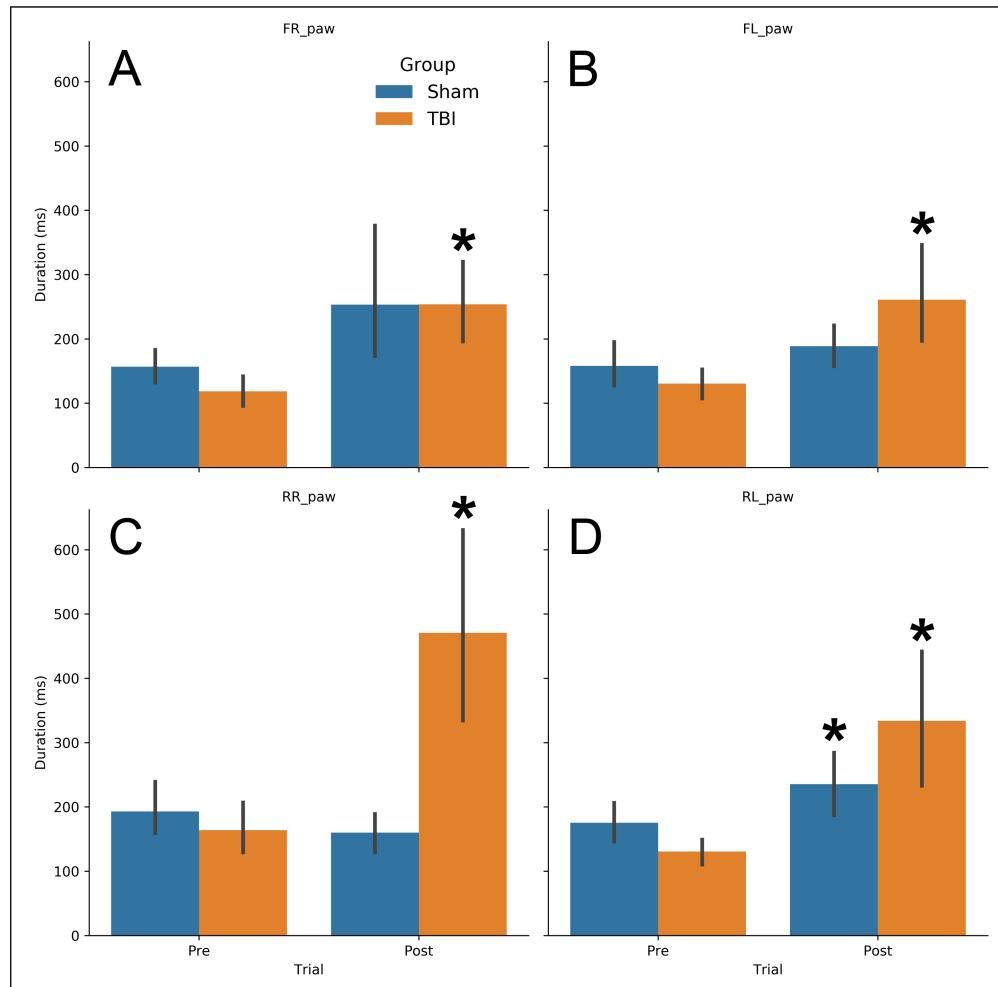


Figure 3.5: Stance phase increased in TBI animals

Stance phase from sham ($n = 3$) and TBI ($n = 3$) animals pre and 30 min post injury. Front right (A), front left (B), and rear right (C) paws increased time of stance phase in TBI animals only ($P = 0.0002$, $P = 0.0022$, and $P = 0.0005$, respectively), while rear left (D) paw stance phase time increased in both sham and TBI animals ($P = 0.0465$ and $P = 0.0011$, respectively).

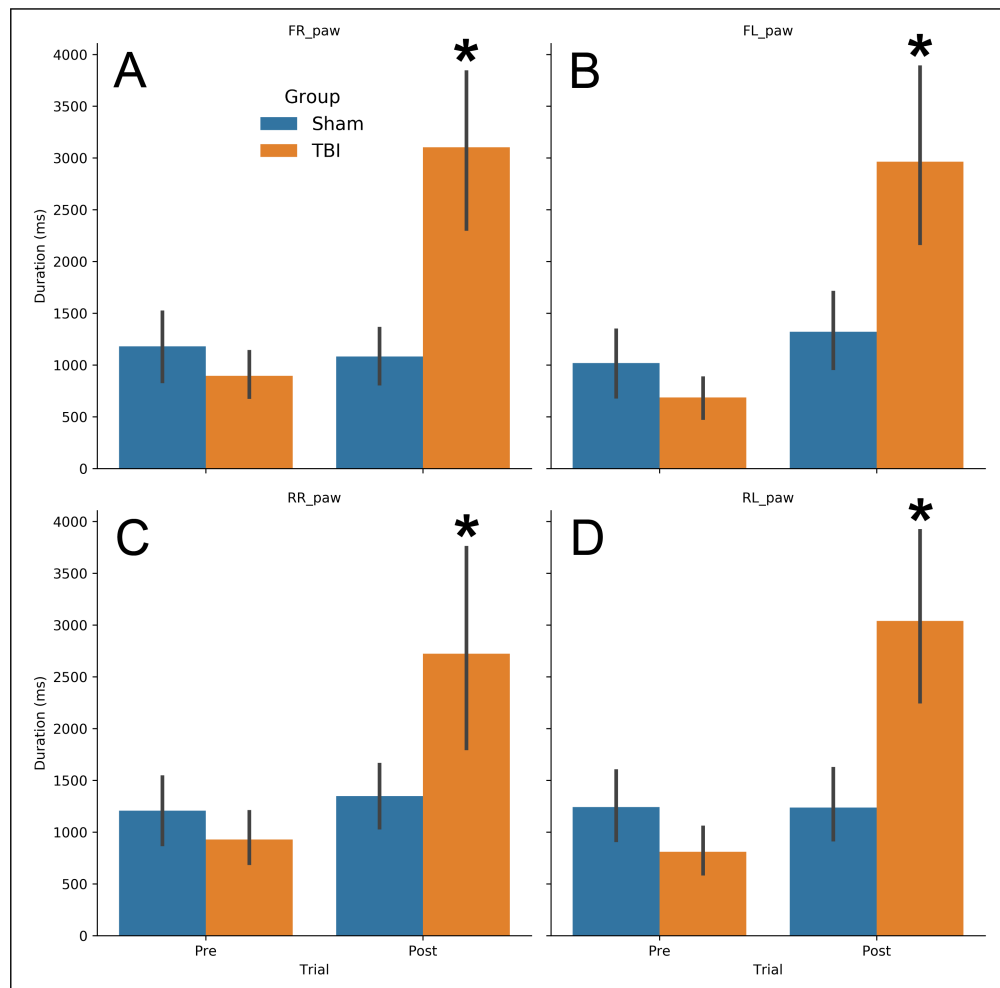


Figure 3.6: Stance phase increased in TBI animals

Swing phase from sham ($n = 3$) and TBI ($n = 3$) animals pre and 30 min post injury. Front right (A), front left (B), rear right (C), and rear left (D) paws increased average swing phase in TBI animals ($P < 0.0001$, $P < 0.0001$, $P = 0.0013$, and $P < 0.0001$, respectively).

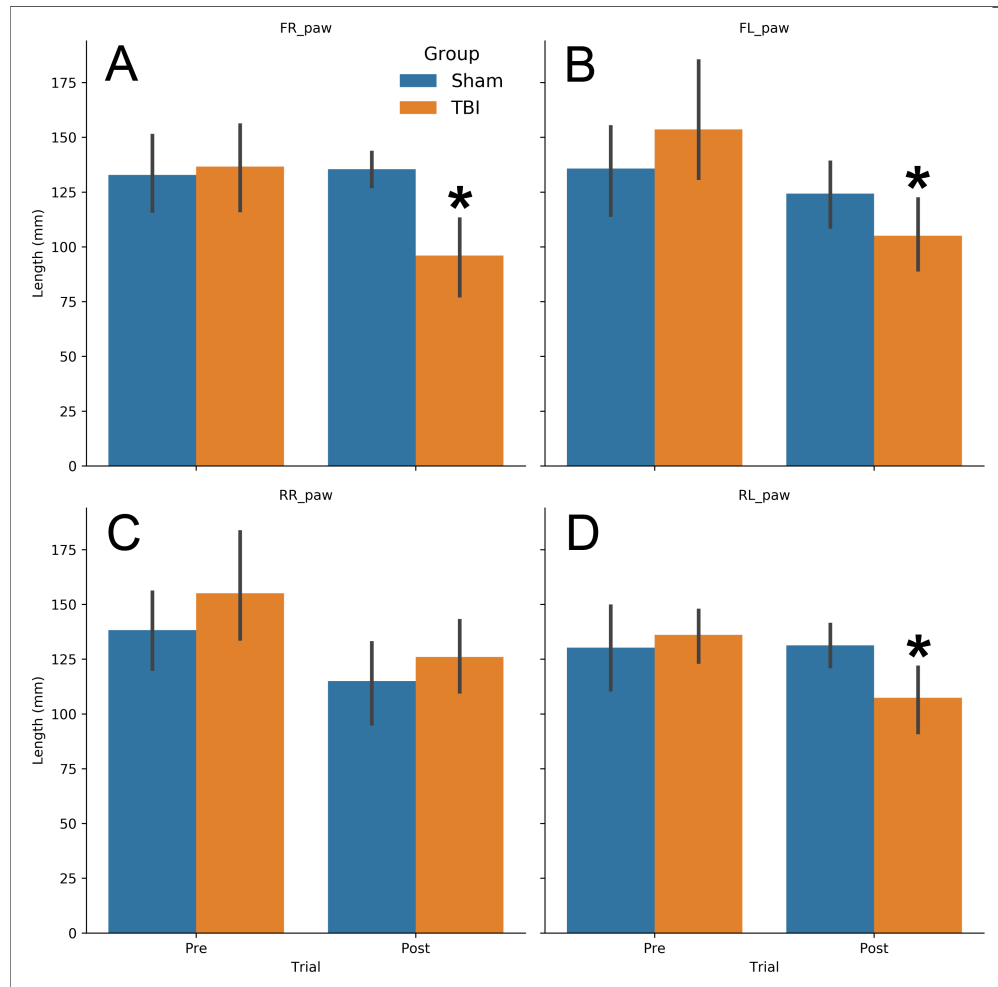


Figure 3.7: Step length decreased in TBI animals

Step length from sham ($n = 3$) and TBI ($n = 3$) animals pre and 30 min post injury. Front right (A), front left (B), and rear left (D) paws increased average step length in TBI animals ($P = 0.0068$, $P = 0.0076$, and $P = 0.0057$, respectively). Rear left (D) paw approached significance in sham ($P = 0.0957$) and rear right (C) approached significance in TBI ($P = 0.0659$).

Chapter 4

Caloric Adequacy and Behavioral Outcomes in a Rat FRCHTBI Model

4.1 Abstract

While changes in global and cerebral metabolism are well documented affects of TBI, nutritional support is often not considered when studying or treating TBI. While some nutritional interventions (notably hypertonic lactate therapy) have emerged, few models exist for studying the role of caloric adequacy in repairing the injured brain. In this work we aimed to create a model for caloric inadequacy in rat TBI adequacy-inadequacy model following FRCHTBI with and without NALAC supplementation as a potential means for exploring the interplay between caloric sufficiency and supplementation. Behavioral evaluation of our rats suggest that our protocol produced a very mild TBI, which was below the detection threshold for most (but not all) metrics used for detection. Unfortunately, this was not a sufficient level of injury to evaluate group differences for the nutritional model introduced. However, the ability of tracking food consumption and LAV to detect changes in appetite and light sensitivity even with mild injury, suggests measures of photosensitivity and food consumption trends should be included in TBI research as a potentially sensitive and clinically relevant assays.

4.2 Introduction

One of the hallmarks of TBI is changes in cerebral metabolism typically marked by a brief hypermetabolic state followed by a more prolonged hypometabolic state lasting weeks or months (Giza and Hovda, 2014; Passineau et al., 2000; Yoshino et al., 1991). Mitochondrial dysfunction, imbalance in fission-fusion dynamics, and elevated reactive oxygen species (ROS) production are central to metabolic and oxidative disruption during this period (Fischer et al., 2016). The magnitude and duration of these mitochondrial and metabolic changes have been tied to injury prognosis (Signoretti et al., 2008; Yokobori et al., 2014) and are

factors in the period of increased vulnerability to exacerbating damage from additional TBI events (Prins et al., 2013; Vagnozzi et al., 2007, 2008). It is therefore crucial to better understand the role of metabolism and nutrition across all severities of TBI to develop functional clinical guidelines to best support the repairing brain.

While lack of appetite is common following even mild TBI, the injured brain requires nutritional support to repair and maintain an anabolic state. The Institute of Medicine Committee on Nutrition, Trauma, and the Brain highlighted the importance of nutritional adequacy (particularly sufficient calories and protein) in the early phases of the injury process (Institute of Medicine (US) Committee on Nutrition, Trauma, and the Brain et al., 2011). Despite this, the current standard of care in many neural ICU provides drastically reduced caloric support resulting in elevated levels of fractional gluconeogenesis (FGNG) indicating a global metabolic crisis with the body mobilizing its glycogen stores to support the injured brain (Glenn et al., 2015a,b).

Lactate therapy has emerged as a promising addition to treatment plans for TBI patients. Lactate can be directly oxidized and is the preferred fuel source of neurons in the brain (Schurr, 2006) and supplementation can help reduce negative outcomes associated with dysfunction in the astrocyte-neuron lactate shuttle (ANLS) (Lama et al., 2014; Patet et al., 2016) while sparing limited cerebral and corporal carbohydrate stores. In addition to a baseline of contributing to gross caloric adequacy, lactate acts as a signalling molecule with anti-inflammatory effects and has been shown to reduce intraperitoneal (IP) (Bouzat et al., 2014).

In this chapter, we evaluate a rat nutritional adequacy-inadequacy model following FRCHTBI with and without NALAC supplementation as a potential means for exploring the interplay between caloric sufficiency and supplementation.

4.3 Methods

An overview of the experimental timeline can be seen in figure 4.1.

Animal Care

All animal procedures were approved by the Animal Care and Use Committee (ACUC) at the University of California Berkeley. Male Sprague Dawley rats were purchased from Charles River USA (Wilmington, MA) at 49 days of age and individually housed. Cages were maintained at a constant temperature and humidity with a 12 hour light-dark cycle (light 7:00 am to 7:00 pm). All animals were given ad lib access to chow for the first 7 days. TBI induction used the same FRCHTBI method and apparatus described in chapter 2, dropping 450g from 135 cm with 3 cm of bolt throw. Following TBI (day 8), animals were

randomly assigned to 5 groups based on injury and nutritional interventions: (1) Sham Injury & ad lib feeding, (2) TBI & ad lib feeding, (3) TBI & half rations, (4) TBI & ad lib feeding with lactate, or (5) TBI & half rations with lactate. A sixth experimental group comprised of animals who died on impact (DOI). Rat and feeding tray weights were recorded daily on a digital scale. Daily food consumption was reported as grams of rat chow and calculated as the delta from the previous days measurement. For half ration groups the average of each rats daily food consumption prior to TBI was calculated and rounded up the nearest half gram to determine their daily allotment. Animals in injection groups were given daily IP injections of 2g/kg NALAC mixed with sterile phosphate buffered saline at a concentration of 200 mg/mL at a pH of 7.4 as in E et al. (2013).

Acute TBI Evaluations

A modified Neurological Severity Score (mNSS) consisting of OF, BW, and IWM tasks was used to evaluate for short term deficits and recovery. All tasks were recorded by a C270 webcams (Logitech, Newark, CA) for later scoring by behavior analysis software (OF) or reported as the average and standard deviation of 2 - 3 scorers blinded to the animals condition (BW and IWM). Scores were recorded approximately an hour before TBI and 30 min, 24 hr, 48 hr, 72 hr, and 240 hr post.

Open Field

Rats were placed in the center of the OF arena measuring 58 x 58 cm and allowed to explore undisturbed for 1 min. Videos were analyzed using Ethovision 15 (NOLDUS; Leesburg, VA) where a 37 x 37 cm center zone and 10.5 x 10.5 cm corner zones were defined. Distance traveled, time in center and corner zones, and frequency of entries to corner zones were calculated.

Beam-Walk

The BW task was administered on 3.8 cm wide by 128 cm long beam with a 20 x 16.5 x 14 cm (depth x width x height) dark box at one end and the exposed portion of beam was marked into four 27 cm sections. Rats were placed at the open end facing the dark box and traversed the beam until entering the box or falling. For two days prior to impact rats were trained on the task until they could complete the task in less than 45 seconds without assistance (up to four trials per day). If the animal failed to complete the task in 45 seconds they were guided to the box and given 30 seconds in the box as recommencement. Time for the animals nose to reach each mark, number of foot faults, partial falls (two limbs off, recovered), and falls were recorded.

Inverted Wire Mesh

Two acrylic frames with external dimensions of 45 x 45 cm and internal dimension of 35 x 35 cm were fastened by bolts to secure 1.25 cm wire mesh for the testing arena. Rats were placed in the center of the wire mesh and once all 4 paws were secure, the arena was inverted by flipping animal head-over-tail over a draped tarp. Time from inversion to release was recorded.

End of Study Behavior Assays

Test of anxiety like behavior (elevated plus maze (EPM)), learning and behavior (Barnes table maze (BTM)), and photosensitivity (LAV) were administered from experimental day 22 - 25 (11 - 14 days post impact) to determine longer lasting effects of TBI and caloric adequacy.

Elevated Plus Maze

The arena was purchased from MazeEngineers (Skokie, IL). It comprised of 4 arms at a right angle, each 50 cm long and 10 cm wide and closed arms had a 40 cm tall wall surrounding them. EPM was administered on experimental day 19 (11 days post impact). Animals were brought into the testing suite at least 30 minutes prior to testing for acclimatization, were placed in the center of the maze facing an open arm, and allowed to explore undisturbed for 5 minutes. Between each trial the arena was cleaned with 0.4% NPD and was fanned dry. Ethovision XT 15 (Noldus; Leesburg, VA) was used to track videos and score time spent in the open arm, frequency of entries into the center zone, open arm, and closed arm, and total distance traveled.

Barnes Table Maze

The arena was purchased from MazeEngineers (Skokie, IL) in black acrylic. It was 122 cm diameter with 20 equally spaced 10 cm diameter holes around the perimeter with a dark escape chamber positioned under one of the holes. An overhead floodlight resulting in intensity measuring 450 lux across the surface and a metronome set to 180 beats per minute at 90 db were provided as aversive stimuli as motivation to find the escape box. Items in the testing remained in identical positions from trial to trial so visual cues would remain consistent. Trials were filmed overhead on a Logitech C270 Webcam (Logitech International; Newark, CA).

BTM was administered on experimental days 19 - 21 (11 - 14 days post TBI). Each day, animals were allowed to acclimatize to the testing suite for 30 minutes. Day 1 consisted of a habituation trial and 2 training trials, with 2 more training trials on day 2, and a memory probe trial on day 3. For the habituation trial, the animal was placed in the center of the arena under a clear container and the metronome was turned on. Each animal was then gently guided to the escape hole and given 3 minutes to enter. If they did not enter with

the container over the hole in this time we placed them in by hand. As soon as the animal entered the escape box the metronome was turned off and the animal was left in the dark box for 1 min before returning to the home cage. For training trials, the animal was placed in the center of the arena and covered by an opaque container before turning on the metronome and removing the container. The rat was given up to 2 minutes to find the escape hole, at which point the clear container was used to gently guide the animal to the escape hole if they had not. As soon as they entered the escape box the metronome was turned off and they were allowed 1 minute in the dark box as reinforcement. For the memory probe trial the escape box was removed and animals were allowed to explore for 2 min. Between each trial the arena surface and escape box were cleaned with 0.4% NPD and fanned dry. Ethovision XT 15 (Noldus; Leesburg, VA) was used to track videos and score latency to escape, distance traveled, errors, and time in the quadrant of the escape hole.

Light Aversion Assay

The LAV was administered and scored as detailed in chapter 3. Briefly, a 50 x 50 x 60 cm (L x W x H) opaque sided OF arena was bisected by an insert to create two 50 x 25 x 60 cm compartments with open access to either via a 10 x 10 cm opening. The dark compartment was covered with opaque lid, while the light compartment was covered by clear acrylic, through which the light intensity was adjusted and filming took place. Animals were acclimatized to the dark environment for 60 min and 5 min trials were administered in ascending intensity (0, 250, 500, and 750 lux) followed by 5 min in their home cage in a dark holding box. Frequency of entries with all 4 limbs and time spent in the light compartment with all 4 limbs was scored.

4.4 Results

Bodyweight and Food Consumption

Bodyweight by group is shown in figure 4.2 A and changed in bodyweight from the previous day is shown in figure 4.2 B. In order to evaluate response of rat weight to the injury and nutritional interventions change in bodyweight was tested for differences between groups at 3 periods: pre-impact (days 1 - 8), 24 hrs post impact (day 9), and post impact recovery (days 10 - 22) (4.1). Pre-impact daily changes in weight showed no group differences (ANOVA $P = 0.9928$). Changes in bodyweight 24 hrs post impact were different for Sham AL - TBI AL ($P = 0.0024$) and Sham AL - TBI Half ($P = 0.0024$), with sham animals gaining 0.83 ± 3.25 g, TBI Half losing 11.8 ± 2.68 g, and TBI AL losing 11 ± 7.16 g. For days 10 - 22 there were differences for comparisons between Sham AL - TBI Half ($P < .0001$) and TBI AL - TBI Half ($P < .0001$) with Sham AL gaining 3.69 ± 3.89 g, TBI AL gaining 3.68 ± 3.47 g, and TBI Half losing 1.22 ± 4.5 g.

Daily food consumption by group is shown in figure 4.2 C and changed in food consumption from the previous day is shown in figure 4.2 D. In order to evaluate response of rat weight to the injury and nutritional interventions change in bodyweight was tested for differences between groups at 3 periods: pre-impact (days 1 - 8), 24 hrs post impact (day 9), and post impact recovery (days 10 - 22) (4.2 and 4.3). Pre-impact (days 1 - 8) there were no differences between groups for daily food consumption (ANOVA $P = 0.2274$) or daily change (ANOVA $P = 0.9377$). In the 24 hours following TBI there were significant differences for food consumption between Sham AL - TBI AL ($P = 0.005836$) and Sham AL - TBI Half ($P = .00034$), as well as daily change between Sham AL - TBI AL ($P = 0.0023$) and Sham AL - TBI Half ($P = 0.002$). For days 10 - 22 there were group differences for food consumption between Sham AL - TBI Half ($P < 0.00001$) and TBI AL - TBI Half ($P < 0.00001$) but not in day to day change in food consumption (ANOVA $P = 0.2732$).

FRCHTBI and injection group exclusion

Of the 29 animals receiving impacts, 7 died before waking from anesthesia. This equates to a 24.14% rate of death from impact. Of the animals who survived post impact, 6 were Sham, 6 TBI AL, 6 TBI Half, 6 TBI AL with Lactate injections, and 5 TBI Half with Lactate injections. However, 2 of the 5 TBI Half Lactate group rats had to be euthanized before the end of study. Due to observed trends in animal weight, stress and health, and behavior trends suggesting reduced activity level in injection groups over the course of the study both ad lib and half ration groups receiving injections were removed from analysis for the study.

Modified NSS

Open Field

Comparisons between time points were made for each group using Repeated Measures Analysis of Variance (RMANOVA) and no differences were detected for total distance traveled (Figure 4.3 A), duration in the center zone (Figure 4.3 B), or duration in the corner zones (Figure 4.3 C).

Beam-Walk

Comparisons between time points were made for each group using RMANOVA and no differences were detected for time to reach the goal box (Figure 4.4 A), footfaults (miss-steps) (Figure 4.4 B), or recovered falls (Figure 4.4 C). No falls were observed.

Inverted Wire Mesh

Comparisons between time points were made for each group using RMANOVA and no differences in IWM hang time were detected (Figure 4.5).

End of Study Behavioral Assays

Elevated Plus Maze

Anxiety like behavior was assessed using the EPM 11 days post impact. Distance travelled in the EPM (Figure 4.6 A) showed no significant differences between groups (ANOVA $P = 0.3649$). Time spent in the open arm (Figure 4.6 B) was not different between Sham - TBI AL, but was greater for TBI Half compared to Sham ($P = 0.0413$) and TBI AL ($P = 0.0418$). Frequency of entries into the open arm (Figure 4.6 C) was not significant for any comparisons (ANOVA $P = 0.0808$), but approached significance for TBI AL - TBI Half ($P = 0.0985$).

Barnes Table Maze

Learning and memory were assessed using a BTM protocol with 2 learning trials each on days 11 and 12 and a memory probe trial on day 13 post TBI. Distance traveled during training trials (Figure 4.7 A) showed no difference between trials for Sham or TBI AL, but was significant for TBI Half for trial 1 - trial 4 ($P = 0.0291$) and approached significance for trial 1 - trial 3 ($P = 0.0742$). Latency to escape (Figure 4.7 B) was significant for TBI Half between trial 1 - trial 4 ($P = 0.011$) and approached significance for Sham between trial 2 - trial 4 ($P = .0965$), for TBI AL between trial 2 - trial 4 ($P = 0.0835$), and for TBI Half between trial 1 - trial 3 ($P = 0.0913$). Primary errors (Figure 4.7 C) showed no significance between trials for any group. No group differences were detected for distance traveled (Figure 4.7 D), latency to find the escape hold (Figure 4.7 E), or primary errors (Figure 4.7 F) during the probe trial.

Light Aversion Assay

LAV was administered 13 days post impact to assess photosensitivity. Frequency of entries into the light compartment (Figure 4.8 A) showed no differences between intensities for sham (ANOVA $P = 0.2817$) and TBI Half (ANOVA $P = 0.1507$). Frequency was significant for TBI AL for 0 - 750 lux ($P = 0.0116$) and approached significance for 0 - 500 lux ($P = 0.944$). Time in the light compartment (Figure 4.8 B) was significantly different for sham for 0 - 750 lux ($P = 0.0195$) and approached significance for 0 - 250 ($P = 0.716$) and 0 - 500 lux ($P = .0707$). For TBI AL time was significantly different for 0 - 250 ($P = 0.49479$), 0 - 500 ($P = 0.0105$), and 0 - 750 lux ($P = 0.0105$). TBI Half showed significance for 0 - 750 lux ($P = 0.0183$).

4.5 Discussion

Acute Post-TBI Changes in Bodyweight and Food Intake Were Driven by TBI, While Differences 24+ hrs After Were Driven by Caloric Intervention

The data presented in figure 4.2 and tables 4.1, 4.2, and 4.3 suggest that trends that are consistent with human reports for concussion. It appears that a drop in food consumption following TBI is more pronounced than in sham regardless of whether animals had ad lib access or only half rations, but quickly recovers for TBI AL animals (Figure 4.2 C and D). This suggests there is an acute and transient reduction of appetite with the impact used in this study, consistent with observations and recommendations from the US Committee on Nutrition, Trauma, and the Brain (Institute of Medicine (US) Committee on Nutrition, Trauma, and the Brain et al., 2011). However, from 24 hrs post TBI through the end of the study Sham AL and TBI AL animals again had similar patterns in food consumption and weight gain, while TBI Half animals showed a steady decline in weight.

Collectively, these data suggest there was a transient reduction of appetite accompanied by acute weight loss following driven by the impact, with a prolonged period of weight loss driven by the caloric reduction. However, it remains unclear whether this period of reduced appetite would be more pronounced or longer lasting in a more severe TBI model. Future TBI studies of various intensities and interventions may consider including bodyweight and food tracking as part of their experimental design to help guide clinical approaches to nutritional recommendations following TBI, which are currently lacking.

Impacts Deficits Were Not Detectable by mNSS Tasks

The mNSS was modified from components of the Boston University Concussion Scale (BUCS) (Tagge, 2016) and was chosen to be consistent with a collaborators lab using the same injury model. Our colleagues mNSS score gave a point for each corner explored in the OF, for each fourth of the BW covered within 45s, and based on hang time for the IWM. However, given the same impact settings (450g from 135cm with 3 cm throw) on an ostensibly similar device, we were unable to reproduce the same level of deficit in the mNSS with this scoring. For this reason, we added more detailed measurements to our analysis for OF (distance traveled and time in zones) and BW (footfaults, partial falls) in hopes to detect effects of our impact. Despite this, neither OF (Figure 4.3), BW (Figure 4.4), nor IWM (Figure 4.5) were able to reliably detect changes over measurement time points, including between pre and 0.5 hr post-TBI.

Photosensitivity Was Detected 13 Days Post Impact

While there were no measurable effects of the TBI in this work on anxiety like behavior or spatial learning detected by EPM (Figure 4.6) or BTM (Figure 4.7), LAV was able to detect an increase in photosensitivity for TBI AL relative to sham (Figure 4.8). This suggests inclusion of measures of sensory sensitivity, a common symptom of human TBI with implications for long term health and quality of life (Callahan and Lim, 2018; Elliott et al., 2018; Shepherd et al., 2020), would be beneficial to include in assessment of intervention efficacy in animal injury models. Importantly, it also shows promise as a measure of long term outcomes or mild injury detection when effects are below the detection threshold of the Glasgow coma scale (GCS). Future work could further explore the degree to which magnitude of sensory sensitivity severity or duration varies with injury severity or type.

Food Seeking Behavior From Half Rations Complicate Behavioral Assay Interpretation

While our hypothesis was that half rations would result in more severe cognitive deficits and photosensitivity than injury alone, TBI Half actually showed slight preference for the light compartment when compared to sham and TBI AL in LAV (Figure 4.8) and an increase in open arm activity in the EPM (Figure 4.6). This could be explained by the food seeking behavior overwriting an increase in discomfort caused by the light, even if an increased photosensitivity did persist as it did in TBI AL. This highlights the importance of choosing tasks which are not reliant on natural avoidance behavior towards bright or open spaces when using models that include caloric restriction as by design interpretation of these results relies on these tendencies for future studies attempting to model caloric deficit during recovery.

Death on Impact Rates

The intent of our injury model was to produce a moderate TBI, and our procedure was reported to produce these effects in the hands of other labs with a similar device. Our post TBI testing did not detect deficits that were suggestive of this level of injury. Despite this, we saw death on impact rates of 24.14% in our injury, consistent with those of our colleagues (25 - 30%) who detected moderate injury (personal correspondence). It is possible midline impacts, such as used in this study, are sensitive to slight deviations in targeting, potentially distributing too much energy to the brainstem or that FRCHTBI models have different phenotypes of rotation that could lead to damage in the spinal cord at a similar percentage despite lower overall level of injury. These targeting data were not available from previous impacts to test this hypothesis.

Injection Group Exclusion

NaLac injection groups were excluded from final analysis due to concerns over health and well-being of the animals and effects of the treatment on their behavior testing, even when they otherwise appeared healthy with monitoring. Of the TBI Half Lactate group, 2 of 5 (40%) had to be euthanized before end of study after showing signs of distress. Additionally, analysis of data from both ad lib and half ration injection groups showed more subtle signs of change over the course of the experiment showing gradual decreases in activity in multiple tasks over time. As such, comparisons were made between caloric adequacy (TBI AL) and inadequacy (TBI Half) in absence of NaLac interventions. Saline injection control cohorts were planned to be included, but the exclusion of these groups prevented that.

Alternative Methods of NaLac Administration

It is possible that the high volume of the IP injections (2.5mL for a 250g rat) given on a daily basis over 2 weeks were too stressful as a procedure either in general, or in conjunction with TBI and / or a half ration diet. The concentration and method of administration for injections used in this study have been used elsewhere (E et al., 2013) for a period of 14 days. However, this was in mice, in the absence of additional stressors (TBI and caloric restriction), and only reported results from biochemical assays. It is therefore possible the different volumes required to reach 2g/kg of NALAC are such that these interventions should not scale directly in this way, that additional stressors may not be compatible with this intervention, or that these deficits were also present in their animals but would not be noticed without tracking bodyweight, food, and frequent measures of activity level.

Additionally, a single bolus delivery may not have the optimal effects of clinical lactate therapies, which are typically applied over a longer time course at a steady rate. Hence, our intervention resulted in a rapid and transient peak in [Lac] and elevated [Gluc] as opposed to a more moderate and sustained elevation of concentration in intravenous (IV) infusion models. Because repeated exposure to anesthesia would confound outcomes, IV is not suited for daily administration in rodents, although studies supplementing with hypertonic NALAC using a single extended IV infusion (3 hrs starting 30 min post TBI) and found beneficial results (Holloway et al., 2007; Millet et al., 2018). A model of administration that includes both extended exposure and frequent administration over time would most accurately mimic potential real-world applications. Future work looking to produce prolonged administration could consider osmotic pump implants to replicate clinical settings, or oral gavage to replicate ingest-able supplementation for conscious individuals to properly account for differences due to the first-pass effect.

4.6 Conclusion

Collectively, the data suggest a very mild TBI resulted from the impact in these animals, which was not well suited to produce deficits severe enough to be exacerbated by a lack of nutritional support for the injured brain. MNSS proved unable to detect deficits, even immediately following TBI and end of study behavior changes appeared to be more driven by food seeking behavior than injury. The ability of tracking food consumption and LAV to detect changes in appetite and light sensitivity due to this mild injury, however, suggests measures of photosensitivity and food consumption trends should be included in TBI research as a potentially sensitive and clinically relevant assays. More consistency and predictability would likely be achieved by a direct-impact FRCHTBI model that does not use a secondary component (in our case a bolt resting on the animals head) to transfer energy from the falling weight by minimizing potential sources of variable energy loss.

4.7 Figures

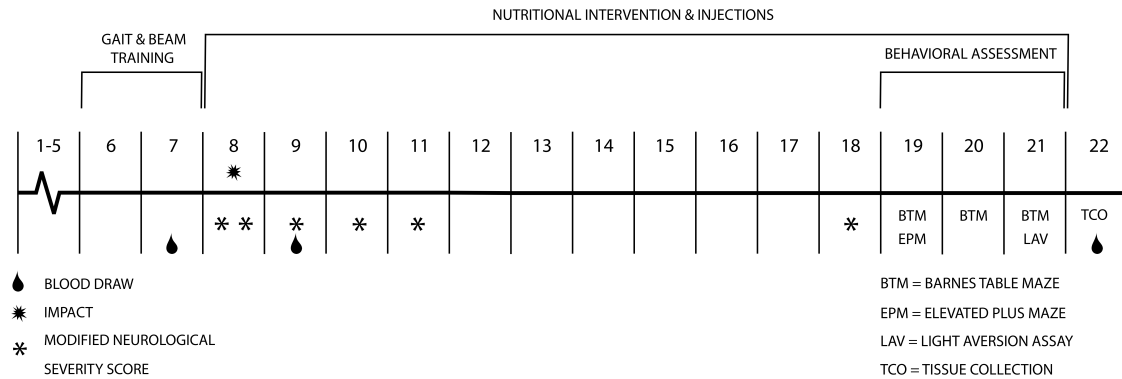


Figure 4.1: Experimental Timeline

Timeline showing the sequence of TBI, behavioral testing, blood collections, and tissue collection. Animal weight and food consumption measurements were taken daily.

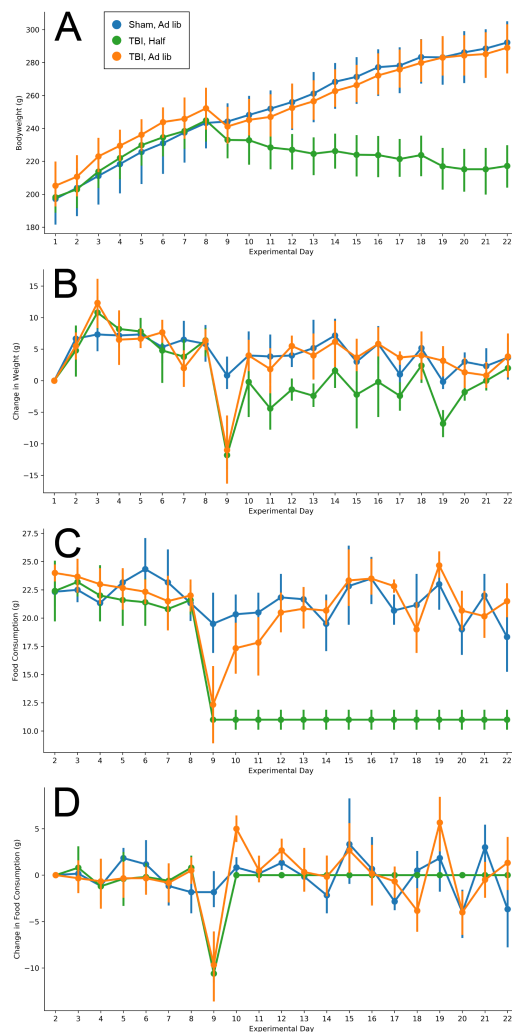


Figure 4.2: Daily bodyweight and food consumption

Daily bodyweight (A) and daily change in bodyweight (B) throughout the study. Daily change was not different between groups pre TBI (days 1 - 8). Changes in bodyweight for the 24 hrs following TBI (day 8 to 9) were different for Sham AL - TBI AL ($P = 0.0024$) and Sham AL - TBI Half ($P = 0.0024$). Changes in bodyweight from days 10 - 22 differed between Sham AL - TBI Half ($P < .0001$) and TBI AL - TBI Half ($P < .0001$). Daily food consumption (C) and daily change in food consumption (D) throughout the study. In the 24 hours following TBI there were significant differences for food consumption between Sham AL - TBI AL ($P = 0.005836$) and Sham AL - TBI Half ($P = .00034$), as well as daily change between Sham AL - TBI AL ($P = 0.0023$) and Sham AL - TBI Half ($P = 0.002$). For days 10 - 22 there were group differences for food consumption between Sham AL - TBI Half ($P < 0.00001$) and TBI AL - TBI Half ($P < 0.00001$).

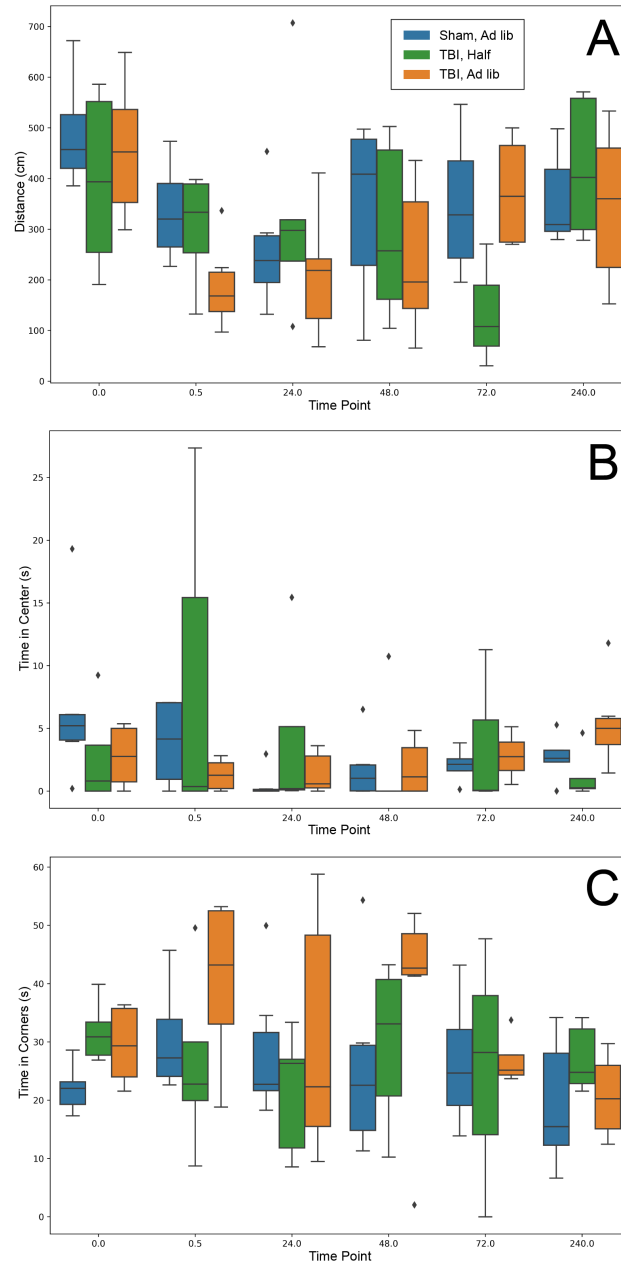


Figure 4.3: open field (OF) performance by group over time

For each measured variable a RMANOVA was run to test for differences between time points for each group. No differences were detected for total distance traveled (A), duration in the center zone (B), or duration in the corner zones (C).

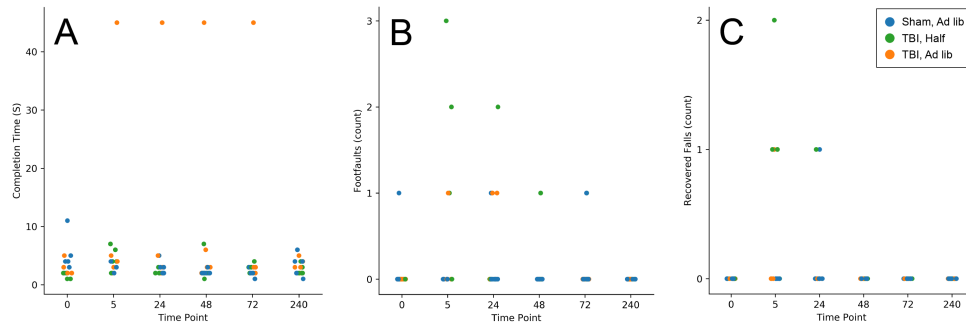


Figure 4.4: beam-walk (BW) performance by group over time
 For each measured variable a RMANOVA was run to test for differences between time points for each group. No differences were detected for time to reach the goal box (A), footfaults (B), or recovered falls (C).

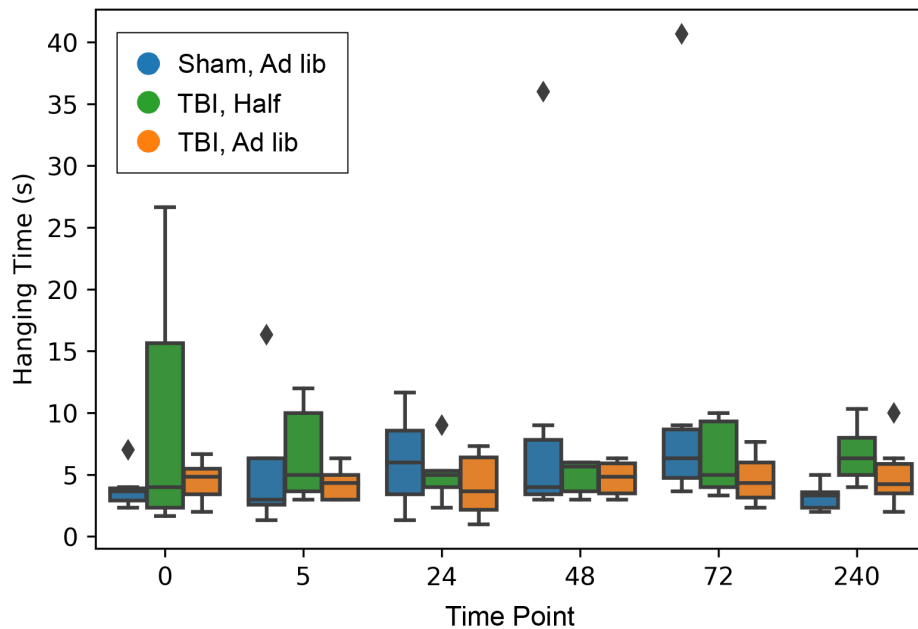


Figure 4.5: Hanging time on inverted wire mesh (IWM).
 Hanging time on the IWM showed no difference between time points for any group.

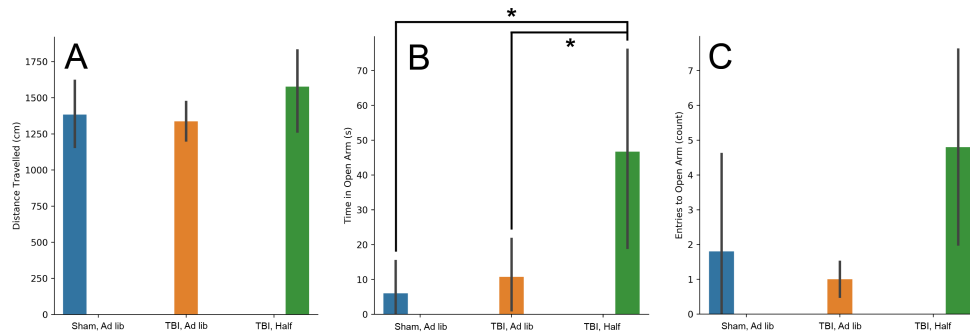


Figure 4.6: elevated plus maze (EPM) performance 10 days post TBI
 Cumulative distance travelled (A) showed no significant differences between groups (ANOVA $P = 0.3649$). Time spent in the open arm (B) was not different between Sham - TBI AL, but was greater for TBI Half compared to Sham ($P = 0.0413$) and TBI AL ($P = 0.0418$). Entries into the open arm (C) was not significant for any comparisons (ANOVA $P = 0.0808$), but approached significance for TBI AL - TBI Half ($P = 0.0985$).

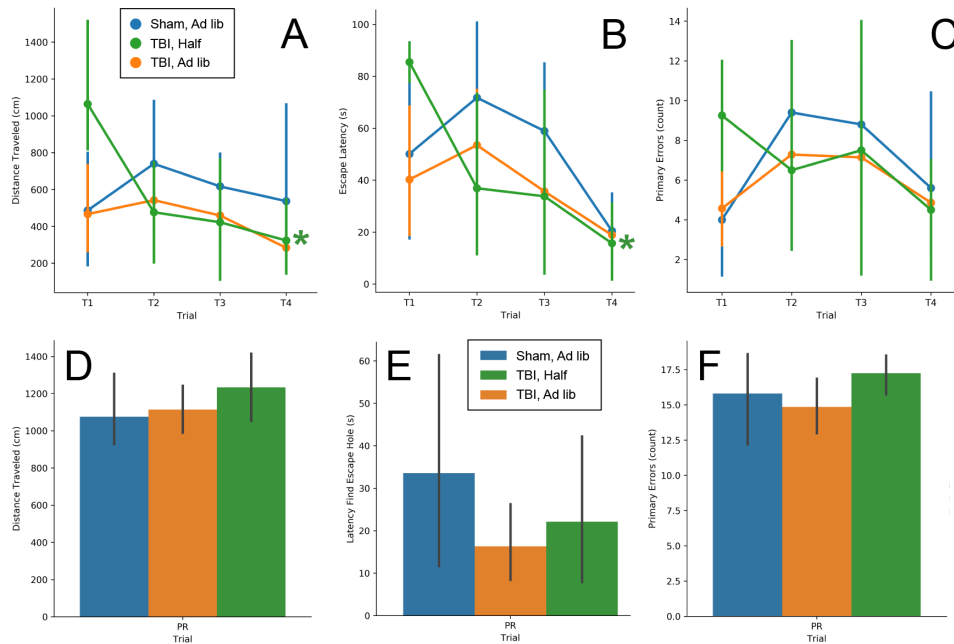


Figure 4.7: acfBTM Performance 11 - 13 days post TBI on training (A - C) and probe (D - F) trials.

For training trials RMANOVA was run for differences between trials for each group. Distance traveled (A) was significant for TBI Half between trial 1 and trial 4 ($P = 0.0291$), latency to escape (B) was significant for TBI Half between trial 1 - trial 4 ($P = 0.011$), and primary errors (C) showed no significance between trials for any group. For the probe trial ANOVA was run for differences between groups. There were no differences between groups for distance traveled (D), latency to find the escape hold (E), or primary errors (F).

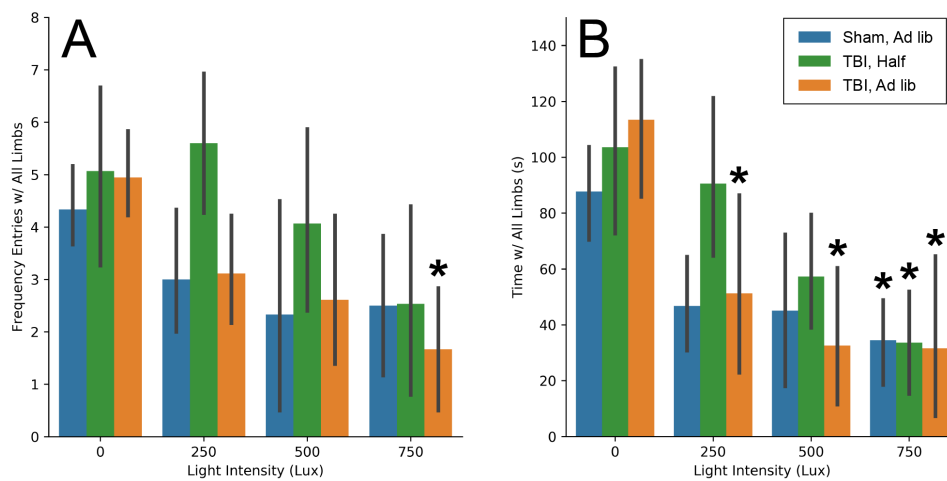


Figure 4.8: light aversion assay (LAV) performance 14 days post TBI

Frequency of entries with all limbs (A) showed no differences between intensities for sham and TBI Half. Frequency was significant for TBI AL for 0 - 750 lux ($P = 0.0116$) and approached significance for 0 - 500 lux ($P = 0.944$). Time in the light compartment (B) was significantly different for sham for 0 - 750 lux ($P = 0.0195$) and approached significance for 0 - 250 ($P = 0.716$) and 0 - 500 lux ($P = .0707$). TBI AL was significantly different for 0 - 250 ($P = 0.49479$), 0 - 500 ($P = 0.0105$), and 0 - 750 lux ($P = 0.0105$). TBI Half showed significance for 0 - 750 lux ($P = 0.0183$).

* significant at $P < 0.5$ compared to 0 lux

		count	mean	std	min	max
Period	Group					
Pre	Sham AL	48.0	5.770833	3.502216	-2.0	11.0
	TBI Half	40.0	5.825000	4.500071	-5.0	14.0
	TBI AL	48.0	5.875000	4.724878	-4.0	18.0
TBI	Sham AL	6.0	0.833333	3.250641	-2.0	7.0
	TBI Half	5.0	-11.800000	2.683282	-14.0	-8.0
	TBI AL	6.0	-11.000000	7.155418	-20.0	-1.0
Post	Sham AL	78.0	3.692308	3.899076	-4.0	13.0
	TBI Half	65.0	-1.215385	4.512110	-12.0	12.0
	TBI AL	78.0	3.679487	3.743370	-6.0	11.0

Table 4.1: Daily change in bodyweight pre, 24 after, and post impact
Average change in rat bodyweight day to day for pre TBI (days 1 - 8), 24 hrs following TBI (day 9), and post TBI recovery (days 10 - 22) by group.

		count	mean	std	min	max
Period	Group					
Pre	Sham AL	42.0	22.595238	2.469912	18.0	30.0
	TBI Half	35.0	21.857143	2.463174	18.0	27.0
	TBI AL	42.0	22.738095	2.130608	18.0	27.0
TBI	Sham AL	6.0	19.500000	3.449638	15.0	25.0
	TBI Half	5.0	11.000000	1.000000	10.0	12.0
	TBI AL	6.0	12.333333	4.546061	7.0	19.0
Post	Sham AL	78.0	21.102564	3.172896	13.0	29.0
	TBI Half	65.0	11.000000	0.901388	10.0	12.0
	TBI AL	78.0	20.987179	3.114664	12.0	29.0

Table 4.2: Daily food consumption pre, 24 after, and post impact
Average food consumption for pre TBI (days 1 - 8), 24 hrs following TBI (day 9), and post
TBI recovery (days 10 - 22) by group.

		count	mean	std	min	max
Period	Group					
Pre	Sham AL	42.0	-0.142857	2.374370	-7.0	6.0
	TBI Half	35.0	-0.114286	2.219849	-5.0	5.0
	TBI AL	42.0	-0.285714	2.266250	-7.0	4.0
TBI	Sham AL	6.0	-1.833333	2.562551	-4.0	3.0
	TBI Half	5.0	-10.600000	0.894427	-12.0	-10.0
	TBI AL	6.0	-9.666667	4.885352	-16.0	-5.0
Post	Sham AL	78.0	-0.089744	4.010330	-10.0	12.0
	TBI Half	65.0	0.000000	0.000000	0.0	0.0
	TBI AL	78.0	0.705128	3.918352	-9.0	11.0

Table 4.3: Daily change in food consumption pre, 24 after, and post impact
Average daily change in food consumption for pre TBI (days 1 - 8), 24 hrs following TBI (day 9), and post TBI recovery (days 10 - 22) by group.

Chapter 5

Conclusions and Future Directions

This work explores methodological approaches to better incorporate kinematic aspects of FRCHTBI models, detect clinically relevant deficits, and model nutritional necessity in repairing the injured brain. While the severity of injury induced in this work did not allow us to produce deficits large enough to measure changes due to nutritional intervention, many aspects of these methods have the capacity to contribute to future understanding of TBI. Importantly these methods focus on low cost, widely available, and open source material and software to lower the barrier of implementation.

FRCHTBI models are more analogous in many ways to commonly occurring forms of human TBI than widely used models. CCI and FPI are much easier to quantify and control input, but make direct contact with the exposed cortex resulting in localized swelling followed by a widespread lesion on the hemisphere receiving impact; properties not common in human CHTBI. While more realistic, weight drop FRCHTBI models inherently contain many sources of variation than can pose problems for injury consistency and analysis. Quantification of the kinematic as well as behavioral and molecular outcomes of these impacts can help confirm consistent injury application, and take sources of variation into account for outcome analysis. Future work should evaluate these properties in their models both within the same injury severity and across the spectrum from mild to severe. In addition to informing research using these models, this would inform approaches to human TBI data collection (using either instrumented equipment or high speed videography) and personal protective equipment design and testing.

LAV was able to detect differences in photosensitivity at sub-acute time points (14 days post impact) in even minor cases of TBI, indicated by the limited effect measured on other behavioral tasks in this study. This could be of importance for mild TBI (concussions), which are by far the most common, especially in instances where individuals are at risk for repeated exposure (e.g. contact sports) leading to second concussion syndrome. This is potentially impactful considering one of, if not the most, widely used field point of care assessments, the GCS, can have a threshold for detection that exceeds minor concussions

(Johnston et al., 2001; McCrory et al., 2013), potentially allowing athletes to return to play and incur another during a crucial window of hyper-vulnerability. Incorporation of LAV testing into future animal TBI research could lead to development of more sensitive and easy to administer field tests, as well as increase our understanding of mechanisms involved in sensory sensitivity and after injury.

Gait analysis was able to detect changes in spatial and temporal gait patterns at acute time points (30 min post impact) in very mild TBI, and could similarly be incorporated into point of care assessment as a stand alone measurement. Indeed, it has been reported in several studies that natural gait patterns in humans are affected acutely following concussion, but are generally recovered at sub-acute time points. The true discriminatory power of gait analysis in clinical TBI is highlighted when combined with dual task assessment, where individuals are asked to complete various cognitive tasks while completing a walking exercise, or complicated gait assessments such as timed heel-toe line walking (reviewed in Fino et al. (2018)). Dual task training has also proven an effective treatment for older adults with and without elevated fear of falling (Falbo et al., 2016; Wollesen et al., 2017) and in patients with various neurological disorders, including TBI (reviewed in Fritz et al. (2015)). While it is not possible to implement a verbal Stroop or serial subtraction task (both commonly used dual task paradigms) with rodents, researchers are finding creative ways to engage animals with challenging cognitively gait tasks (such as running on exercise wheels with missing rungs) that have shown to improve synaptogenesis, angiogenesis, and functional outcomes (reviewed in Jakowec et al. (2016)).

Despite the mild nature of the TBI induced in this work not being suitable to evaluating our caloric adequacy-inadequacy model, these methods of TBI detection showed promise in a common injury severity (i.e. mild concussions) at both acute and sub-acute time points. This has the potential to inform components of field based and clinical point of care assessment, as well as long term symptom severity tracking for lingering sensory sensitivity issues. The ability of these tests, selected based on symptoms commonly presenting in human TBI populations, highlight the importance of using clinically relevant assays for animal models to effectively measure behavioral outcomes with intervention.

Bibliography

Alao, T. and M. Waseem

2020. Penetrating head trauma. In *StatPearls*. Treasure Island (FL): StatPearls Publishing.

Albert-Weissenberger, C. and A.-L. Sirén

2010. Experimental traumatic brain injury. *Exp. Transl. Stroke Med.*, 2(1):16.

Amyot, F., K. Kenney, C. Moore, M. Haber, L. C. Turtzo, C. Shenouda, E. Silverman, Y. Gong, B.-X. Qu, L. Harburg, H. Y. Lu, E. M. Wassermann, and R. Diaz-Arrastia

2018. Imaging of cerebrovascular function in chronic traumatic brain injury. *J. Neurotrauma*, 35(10):1116–1123.

Arshad, Q., R. E. Roberts, H. Ahmad, R. Lobo, M. Patel, T. Ham, D. J. Sharp, and B. M. Seemungal

2017. Patients with chronic dizziness following traumatic head injury typically have multiple diagnoses involving combined peripheral and central vestibular dysfunction. *Clin. Neurol. Neurosurg.*, 155:17–19.

Ashbaugh, A. and C. McGrew

2016. The role of nutritional supplements in sports concussion treatment. *Curr. Sports Med. Rep.*, 15(1):16–19.

Basford, J. R., L.-S. Chou, K. R. Kaufman, R. H. Brey, A. Walker, J. F. Malec, A. M. Moessner, and A. W. Brown

2003. An assessment of gait and balance deficits after traumatic brain injury. *Arch. Phys. Med. Rehabil.*, 84(3):343–349.

Bazarian, J. J., J. McClung, Y. T. Cheng, W. Flesher, and S. M. Schneider

2005. Emergency department management of mild traumatic brain injury in the USA. *Emerg. Med. J.*, 22(7):473–477.

Bland, D. C., C. Zampieri, and D. L. Damiano

2011. Effectiveness of physical therapy for improving gait and balance in individuals with traumatic brain injury: a systematic review. *Brain Inj.*, 25(7-8):664–679.

- Bodnar, C. N., K. N. Roberts, E. K. Higgins, and A. D. Bachstetter
2019. A systematic review of closed head injury models of mild traumatic brain injury in mice and rats. *J. Neurotrauma*, 36(11):1683–1706.
- Bohnen, N., A. Twijnstra, G. Wijnen, and J. Jolles
1991. Tolerance for light and sound of patients with persistent post-concussional symptoms 6 months after mild head injury. *J. Neurol.*, 238(8):443–446.
- Bouzat, P., N. Sala, T. Suys, J.-B. Zerlauth, P. Marques-Vidal, F. Feihl, J. Bloch, M. Messerer, M. Levivier, R. Meuli, P. J. Magistretti, and M. Oddo
2014. Cerebral metabolic effects of exogenous lactate supplementation on the injured human brain. *Intensive Care Med.*, 40(3):412–421.
- Bramlett, H. M. and W. D. Dietrich
2015. Long-Term consequences of traumatic brain injury: Current status of potential mechanisms of injury and neurological outcomes. *J. Neurotrauma*, 32(23):1834–1848.
- Callahan, M. L. and M. M. Lim
2018. Sensory sensitivity in TBI: Implications for chronic disability. *Curr. Neurol. Neurosci. Rep.*, 18(9):56.
- CDC
2019. Surveillance report of traumatic brain injury-related emergency department visits, hospitalizations, and deaths - united states, 2014. Technical report, Centers for Disease Control and Prevention, U.S. Department of Health and Human Services.
- Corso, P., E. Finkelstein, T. Miller, I. Fiebelkorn, and E. Zaloshnja
2006. Incidence and lifetime costs of injuries in the united states. *Inj. Prev.*, 12(4):212–218.
- Daneshvar, D. H., D. O. Riley, C. J. Nowinski, A. C. McKee, R. A. Stern, and R. C. Cantu
2011. Long-term consequences: effects on normal development profile after concussion. *Phys. Med. Rehabil. Clin. N. Am.*, 22(4):683–700, ix.
- Dikmen, S., J. Machamer, J. R. Fann, and N. R. Temkin
2010. Rates of symptom reporting following traumatic brain injury. *J. Int. Neuropsychol. Soc.*, 16(3):401–411.
- Dixon, C. E., G. L. Clifton, J. W. Lighthall, A. A. Yaghmai, and R. L. Hayes
1991. A controlled cortical impact model of traumatic brain injury in the rat. *J. Neurosci. Methods*, 39(3):253–262.
- Dixon, C. E., B. G. Lyeth, J. T. Povlishock, R. L. Findling, R. J. Hamm, A. Marmarou, H. F. Young, and R. L. Hayes
1987. A fluid percussion model of experimental brain injury in the rat. *J. Neurosurg.*, 67(1):110–119.

- E, L., J. Lu, J. E. Selfridge, J. M. Burns, and R. H. Swerdlow
2013. Lactate administration reproduces specific brain and liver exercise-related changes. *J. Neurochem.*, 127(1):91–100.
- Elliott, J. E., R. A. Opel, K. B. Weymann, A. Q. Chau, M. A. Papesh, M. L. Callahan, D. Storzbach, and M. M. Lim
2018. Sleep disturbances in traumatic brain injury: Associations with sensory sensitivity. *J. Clin. Sleep Med.*, 14(7):1177–1186.
- Falbo, S., G. Condello, L. Capranica, R. Forte, and C. Pesce
2016. Effects of Physical-Cognitive dual task training on executive function and gait performance in older adults: A randomized controlled trial. *Biomed Res. Int.*, 2016:5812092.
- Faul, M. and V. Coronado
2015. Epidemiology of traumatic brain injury. *Handb. Clin. Neurol.*, 127:3–13.
- Feeney, D. M., M. G. Boyeson, R. T. Linn, H. M. Murray, and W. G. Dail
1981. Responses to cortical injury: I. methodology and local effects of contusions in the rat. *Brain Res.*, 211(1):67–77.
- Finkelstein, E., P. S. Corso, and T. R. Miller
2006. *The Incidence and Economic Burden of Injuries in the United States*. Oxford University Press.
- Fino, P. C., L. Parrington, W. Pitt, D. N. Martini, J. C. Chesnutt, L.-S. Chou, and L. A. King
2018. Detecting gait abnormalities after concussion or mild traumatic brain injury: A systematic review of single-task, dual-task, and complex gait. *Gait Posture*, 62:157–166.
- Fischer, T. D., M. J. Hylin, J. Zhao, A. N. Moore, M. N. Waxham, and P. K. Dash
2016. Altered mitochondrial dynamics and TBI pathophysiology. *Front. Syst. Neurosci.*, 10:29.
- Foda, M. A. and A. Marmarou
1994. A new model of diffuse brain injury in rats. part II: Morphological characterization. *J. Neurosurg.*, 80(2):301–313.
- Fritz, N. E., F. M. Cheek, and D. S. Nichols-Larsen
2015. Motor-Cognitive Dual-Task training in persons with neurologic disorders: A systematic review. *J. Neurol. Phys. Ther.*, 39(3):142–153.
- Giza, C. C. and D. A. Hovda
2014. The new neurometabolic cascade of concussion. *Neurosurgery*, 75 Suppl 4:S24–33.

- Glenn, T. C., N. A. Martin, M. A. Horning, D. L. McArthur, D. A. Hovda, P. Vespa, and G. A. Brooks
2015a. Lactate: brain fuel in human traumatic brain injury: a comparison with normal healthy control subjects. *J. Neurotrauma*, 32(11):820–832.
- Glenn, T. C., N. A. Martin, D. L. McArthur, D. A. Hovda, P. Vespa, M. L. Johnson, M. A. Horning, and G. A. Brooks
2015b. Endogenous nutritive support after traumatic brain injury: Peripheral lactate production for glucose supply via gluconeogenesis. *J. Neurotrauma*, 32(11):811–819.
- Gonzalez Tortosa, J., J. F. Martínez-Lage, and M. Poza
2004. Bitemporal head crush injuries: clinical and radiological features of a distinctive type of head injury. *J. Neurosurg.*, 100(4):645–651.
- Holloway, R., Z. Zhou, H. B. Harvey, J. E. Levasseur, A. C. Rice, D. Sun, R. J. Hamm, and M. R. Bullock
2007. Effect of lactate therapy upon cognitive deficits after traumatic brain injury in the rat. *Acta Neurochir.*, 149(9):919–27; discussion 927.
- Hyder, A. A., C. A. Wunderlich, P. Puvanachandra, G. Gururaj, and O. C. Kobusingye
2007. The impact of traumatic brain injuries: a global perspective. *NeuroRehabilitation*, 22(5):341–353.
- Institute of Medicine (US) Committee on Nutrition, Trauma, and the Brain, J. Erdman, M. Oria, and L. Pillsbury
2011. *COMMITTEE ON NUTRITION, TRAUMA, AND THE BRAIN*. National Academies Press (US).
- Jacobs, B. Y., E. H. Lakes, A. J. Reiter, S. P. Lake, T. R. Ham, N. D. Leipzig, S. L. Porvasnik, C. E. Schmidt, R. A. Wachs, and K. D. Allen
2018. The open source GAITOR suite for rodent gait analysis. *Sci. Rep.*, 8(1):9797.
- Jakowec, M. W., Z. Wang, D. Holschneider, J. Beeler, and G. M. Petzinger
2016. Engaging cognitive circuits to promote motor recovery in degenerative disorders. exercise as a learning modality. *J. Hum. Kinet.*, 52:35–51.
- Johnston, K. M., P. McCrory, N. G. Mohtadi, and W. Meeuwisse
2001. Evidence-Based review of sport-related concussion: clinical science. *Clin. J. Sport Med.*, 11(3):150–159.
- Kane, M. J., M. Angoa-Pérez, D. I. Briggs, D. C. Viano, C. W. Kreipke, and D. M. Kuhn
2012. A mouse model of human repetitive mild traumatic brain injury. *J. Neurosci. Methods*, 203(1):41–49.

Kleiven, S.

2013. Why most traumatic brain injuries are not caused by linear acceleration but skull fractures are. *Front Bioeng Biotechnol*, 1:15.

Kumar, A. and D. J. Loane

2012. Neuroinflammation after traumatic brain injury: opportunities for therapeutic intervention. *Brain Behav. Immun.*, 26(8):1191–1201.

Lama, S., R. N. Auer, R. Tyson, C. N. Gallagher, B. Tomanek, and G. R. Sutherland

2014. Lactate storm marks cerebral metabolism following brain trauma. *J. Biol. Chem.*, 289(29):20200–20208.

Langlois, J. A., W. Rutland-Brown, and M. M. Wald

2006. The epidemiology and impact of traumatic brain injury: a brief overview. *J. Head Trauma Rehabil.*, 21(5):375–378.

Ma, X., A. Aravind, B. J. Pfister, N. Chandra, and J. Haorah

2019. Animal models of traumatic brain injury and assessment of injury severity. *Mol. Neurobiol.*, 56(8):5332–5345.

Maas, A. I. R., D. K. Menon, P. D. Adelson, N. Andelic, M. J. Bell, A. Belli, P. Bragge, A. Brazinova, A. Büki, R. M. Chesnut, G. Citerio, M. Coburn, D. J. Cooper, A. T. Crowder, E. Czeiter, M. Czosnyka, R. Diaz-Arrastia, J. P. Dreier, A.-C. Duhaime, A. Ercole, T. A. van Essen, V. L. Feigin, G. Gao, J. Giacino, L. E. Gonzalez-Lara, R. L. Gruen, D. Gupta, J. A. Hartings, S. Hill, J.-Y. Jiang, N. Ketharanathan, E. J. O. Kompanje, L. Lanyon, S. Laureys, F. Lecky, H. Levin, H. F. Lingsma, M. Maegele, M. Majdan, G. Manley, J. Marsteller, L. Mascia, C. McFadyen, S. Mondello, V. Newcombe, A. Palotie, P. M. Parizel, W. Peul, J. Piercy, S. Polinder, L. Puybasset, T. E. Rasmussen, R. Rossaint, P. Smielewski, J. Söderberg, S. J. Stanworth, M. B. Stein, N. von Steinbüchel, W. Stewart, E. W. Steyerberg, N. Stocchetti, A. Synnot, B. Te Ao, O. Tenovuo, A. Theadom, D. Tibboel, W. Videtta, K. K. W. Wang, W. H. Williams, L. Wilson, K. Yaffe, and InTBIR Participants and Investigators

2017. Traumatic brain injury: integrated approaches to improve prevention, clinical care, and research. *Lancet Neurol.*, 16(12):987–1048.

Marcus, H. J., H. Paine, M. Sargeant, S. Wolstenholme, K. Collins, N. Marroney, Q. Arshad, K. Tsang, B. Jones, R. Smith, M. H. Wilson, H. M. Rust, and B. M. Seemungal

2019. Vestibular dysfunction in acute traumatic brain injury. *J. Neurol.*, 266(10):2430–2433.

Marmarou, A., M. A. Foda, W. van den Brink, J. Campbell, H. Kita, and K. Demetriadou

1994. A new model of diffuse brain injury in rats. part i: Pathophysiology and biomechanics. *J. Neurosurg.*, 80(2):291–300.

- Maruichi, K., S. Kuroda, Y. Chiba, M. Hokari, H. Shichinohe, K. Hida, and Y. Iwasaki
2009. Graded model of diffuse axonal injury for studying head injury-induced cognitive dysfunction in rats. *Neuropathology*, 29(2):132–139.
- Masel, B. E. and D. S. DeWitt
2010. Traumatic brain injury: a disease process, not an event. *J. Neurotrauma*, 27(8):1529–1540.
- Mathis, A., P. Mamidanna, K. M. Cury, T. Abe, V. N. Murthy, M. W. Mathis, and M. Bethge
2018. DeepLabCut: markerless pose estimation of user-defined body parts with deep learning. *Nat. Neurosci.*, 21(9):1281–1289.
- McCrorry, P., W. H. Meeuwisse, M. Aubry, R. C. Cantu, J. Dvořák, R. J. Echemendia, L. Engebretsen, K. M. Johnston, J. S. Kutcher, M. Raftery, A. Sills, B. W. Benson, G. A. Davis, R. Ellenbogen, K. M. Guskiewicz, S. A. Herring, G. L. Iverson, B. D. Jordan, J. Kissick, M. McCrea, A. S. McIntosh, D. L. Maddocks, M. Makdissi, L. Purcell, M. Putukian, K. Schneider, C. H. Tator, and M. Turner
2013. Consensus statement on concussion in sport—the 4th international conference on concussion in sport held in zurich, november 2012. *PM R*, 5(4):255–279.
- McIntosh, T. K., L. Noble, B. Andrews, and A. I. Faden
1987. Traumatic brain injury in the rat: characterization of a midline fluid-percussion model. *Cent. Nerv. Syst. Trauma*, 4(2):119–134.
- Mendes, C. S., I. Bartos, Z. Márka, T. Akay, S. Márka, and R. S. Mann
2015. Quantification of gait parameters in freely walking rodents. *BMC Biol.*, 13:50.
- Millet, A., A. Cuisinier, P. Bouzat, C. Batandier, B. Lemasson, V. Stupar, K. Pernet-Gallay, T. Crespy, E. L. Barbier, and J. F. Payen
2018. Hypertonic sodium lactate reverses brain oxygenation and metabolism dysfunction after traumatic brain injury. *Br. J. Anaesth.*, 120(6):1295–1303.
- Namjoshi, D. R., C. Good, W. H. Cheng, W. Panenka, D. Richards, P. A. Cripton, and C. L. Wellington
2013. Towards clinical management of traumatic brain injury: a review of models and mechanisms from a biomechanical perspective. *Dis. Model. Mech.*, 6(6):1325–1338.
- Neumann, M., Y. Wang, S. Kim, S. M. Hong, L. Jeng, M. Bilgen, and J. Liu
2009. Assessing gait impairment following experimental traumatic brain injury in mice. *J. Neurosci. Methods*, 176(1):34–44.
- Orendorff, R., A. J. Peck, B. Zheng, S. N. Shirazi, R. Matthew Ferguson, A. P. Khandhar, S. J. Kemp, P. Goodwill, K. M. Krishnan, G. A. Brooks, D. Kaufer, and S. Conolly
2017. First in vivo traumatic brain injury imaging via magnetic particle imaging. *Phys. Med. Biol.*, 62(9):3501–3509.

- Passineau, M. J., W. Zhao, R. Busto, W. D. Dietrich, O. Alonso, J. Y. Loor, H. M. Bramlett, and M. D. Ginsberg
2000. Chronic metabolic sequelae of traumatic brain injury: prolonged suppression of somatosensory activation. *Am. J. Physiol. Heart Circ. Physiol.*, 279(3):H924–31.
- Patet, C., T. Suys, L. Carteron, and M. Oddo
2016. Cerebral lactate metabolism after traumatic brain injury. *Curr. Neurol. Neurosci. Rep.*, 16(4):31.
- Prins, M. L., D. Alexander, C. C. Giza, and D. A. Hovda
2013. Repeated mild traumatic brain injury: mechanisms of cerebral vulnerability. *J. Neurotrauma*, 30(1):30–38.
- Roozenbeek, B., A. I. R. Maas, and D. K. Menon
2013. Changing patterns in the epidemiology of traumatic brain injury. *Nat. Rev. Neurol.*, 9(4):231–236.
- Rosenfeld, J. V., A. C. McFarlane, P. Bragge, R. A. Armonda, J. B. Grimes, and G. S. Ling
2013. Blast-related traumatic brain injury. *Lancet Neurol.*, 12(9):882–893.
- Row, J., L. Chan, D. Damiano, C. Shenouda, J. Collins, and C. Zampieri
2019. Balance assessment in traumatic brain injury: A comparison of the sensory organization and limits of stability tests. *J. Neurotrauma*, 36(16):2435–2442.
- Rowson, S., S. M. Duma, J. G. Beckwith, J. J. Chu, R. M. Greenwald, J. J. Crisco, P. G. Brolinson, A.-C. Duhaime, T. W. McAllister, and A. C. Maerlender
2012. Rotational head kinematics in football impacts: an injury risk function for concussion. *Ann. Biomed. Eng.*, 40(1):1–13.
- Sanderson, W. C., S. Scherbov, and P. Gerland
2017. Probabilistic population aging. *PLoS One*, 12(6):e0179171.
- Schneider, C. A., W. S. Rasband, and K. W. Eliceiri
2012. NIH image to ImageJ: 25 years of image analysis. *Nat. Methods*, 9(7):671–675.
- Schurr, A.
2006. Lactate: the ultimate cerebral oxidative energy substrate? *J. Cereb. Blood Flow Metab.*, 26(1):142–152.
- Seabold, S. and J. Perktold
2010. Statsmodels: Econometric and statistical modeling with python. In *9th Python in Science Conference*.
- Shepherd, D., J. Landon, M. Kalloor, S. Barker-Collo, N. Starkey, K. Jones, S. Ameratunga, A. Theadom, and BIONIC Research Group
2020. The association between health-related quality of life and noise or light sensitivity in survivors of a mild traumatic brain injury. *Qual. Life Res.*, 29(3):665–672.

- Signoretti, S., A. Marmarou, G. A. Aygok, P. P. Fatouros, G. Portella, and R. M. Bullock
2008. Assessment of mitochondrial impairment in traumatic brain injury using high-resolution proton magnetic resonance spectroscopy. *J. Neurosurg.*, 108(1):42–52.
- Smith, D. H., H. D. Soares, J. S. Pierce, K. G. Perlman, K. E. Saatman, D. F. Meaney, C. E. Dixon, and T. K. McIntosh
1995. A model of parasagittal controlled cortical impact in the mouse: cognitive and histopathologic effects. *J. Neurotrauma*, 12(2):169–178.
- Sullivan, P. G., J. D. Geiger, M. P. Mattson, and S. W. Scheff
2000. Dietary supplement creatine protects against traumatic brain injury. *Ann. Neurol.*, 48(5):723–729.
- Tagge, C. A.
2016. *Effects of concussive impact injury assessed in a new murine neurotrauma model*. PhD thesis, Boston University.
- Talavage, T. M., E. A. Nauman, E. L. Breedlove, U. Yoruk, A. E. Dye, K. E. Morigaki, H. Feuer, and L. J. Leverenz
2014. Functionally-detected cognitive impairment in high school football players without clinically-diagnosed concussion. *J. Neurotrauma*, 31(4):327–338.
- Thiels, E., E. K. Hoffman, and M. B. Gorin
2008. A reliable behavioral assay for the assessment of sustained photophobia in mice. *Curr. Eye Res.*, 33(5):483–491.
- Trojian, T. H., D. H. Wang, and J. J. Leddy
2017. Nutritional supplements for the treatment and prevention of Sports-Related Concussion-Evidence still lacking. *Curr. Sports Med. Rep.*, 16(4):247–255.
- Ustinova, K. I., L. A. Chernikova, A. Dull, and J. Perkins
2015. Physical therapy for correcting postural and coordination deficits in patients with mild-to-moderate traumatic brain injury. *Physiother. Theory Pract.*, 31(1):1–7.
- Vagnozzi, R., S. Signoretti, B. Tavazzi, R. Floris, A. Ludovici, S. Marziali, G. Tarascio, A. M. Amorini, V. Di Pietro, R. Delfini, and G. Lazzarino
2008. Temporal window of metabolic brain vulnerability to concussion: a pilot 1h-magnetic resonance spectroscopic study in concussed athletes—part III. *Neurosurgery*, 62(6):1286–95; discussion 1295–6.
- Vagnozzi, R., B. Tavazzi, S. Signoretti, A. M. Amorini, A. Belli, M. Cimatti, R. Delfini, V. Di Pietro, A. Finocchiaro, and G. Lazzarino
2007. Temporal window of metabolic brain vulnerability to concussions: mitochondrial-related impairment—part I. *Neurosurgery*, 61(2):379–88; discussion 388–9.

- Veksler, R., U. Vazana, Y. Serlin, O. Prager, J. Ofer, N. Shemen, A. M. Fisher, O. Minaeva, N. Hua, R. Saar-Ashkenazy, I. Benou, T. Riklin-Raviv, E. Parker, G. Mumby, L. Kamintsky, S. Beyea, C. V. Bowen, I. Shelef, E. O’Keeffe, M. Campbell, D. Kaufer, L. E. Goldstein, and A. Friedman
2020. Slow blood-to-brain transport underlies enduring barrier dysfunction in american football players. *Brain*, 143(6):1826–1842.
- Vlček, M., E. Jaganjac, M. Niedoba, I. Landor, and J. Neumann
2018. Current treatment procedures for civilian gunshot wounds. *Rozhl. Chir.*, 97(12):558–562.
- Waddell, P. A. and D. M. Gronwall
1984. Sensitivity to light and sound following minor head injury. *Acta Neurol. Scand.*, 69(5):270–276.
- Williams, G., M. E. Morris, A. Schache, and P. R. McCrory
2009. Incidence of gait abnormalities after traumatic brain injury. *Arch. Phys. Med. Rehabil.*, 90(4):587–593.
- Williams, G., A. Schache, and M. E. Morris
2013. Running abnormalities after traumatic brain injury. *Brain Inj.*, 27(4):434–443.
- Wilson, L., W. Stewart, K. Dams-O’Connor, R. Diaz-Arrastia, L. Horton, D. K. Menon, and S. Polinder
2017. The chronic and evolving neurological consequences of traumatic brain injury. *Lancet Neurol.*, 16(10):813–825.
- Wollesen, B., S. Schulz, L. Seydell, and K. Delbaere
2017. Does dual task training improve walking performance of older adults with concern of falling? *BMC Geriatr.*, 17(1):213.
- Yokobori, S., A. T. Mazzeo, S. Gajavelli, and M. R. Bullock
2014. Mitochondrial neuroprotection in traumatic brain injury: rationale and therapeutic strategies. *CNS Neurol. Disord. Drug Targets*, 13(4):606–619.
- Yoshino, A., D. A. Hovda, T. Kawamata, Y. Katayama, and D. P. Becker
1991. Dynamic changes in local cerebral glucose utilization following cerebral concussion in rats: evidence of a hyper- and subsequent hypometabolic state. *Brain Res.*, 561(1):106–119.
- Yu, J., H. Zhu, S. Taheri, W. Mondy, S. Perry, and M. S. Kindy
2018. Impact of nutrition on inflammation, tauopathy, and behavioral outcomes from chronic traumatic encephalopathy. *J. Neuroinflammation*, 15(1):277.